January 2023

Pilot scale Bioreactors at Eagle Gold Mine site:

Studying bacterial populations' adaption to seasonal freeze and thaw cycles and their capacity to remove Sb, Se and As.

Yukon University

Project team:

Dr. Guillaume Nielsen, IRC in NMR, Yukon U

Ben McGrath, Laboratory Technician, Yukon U

Morgan Gilmar, Research Assistant, Yukon U

Chelsey Zurkan, Research Assistant, Yukon U

Ingrid Janzen, Research Assistant, Yukon U

Reanna Moore, Research Assistant, Yukon U

Inderjeet Kaur, Student Proctor, Yukon U

Dr. Morgane Desmau, Postdoctoral Fellow NMR, Yukon U

Acknowledgment:

We would like to thank Natural Sciences and Engineering Research Council of Canada (NSERC) for supporting the Industrial Research Chair in Northern Mine Remediation.

We also would like to thank Victoria Gold Staff for their amazing support on site and for their expertise that helped to conduct this pilot scale experiment.

This publication may be obtained online at yukonu.ca/research

This publication may be obtained from:

YukonU Research Centre, Yukon University
520 University Drive
P.O. Box 2799,
Whitehorse, Yukon
Y1A 5K4
(867) 668-8895
1-800-661-0504
yukonu.ca/research

Table of Contents

Figures:

Tables

Acronyms:

AMD	acid mine drainage
As	Arsenic
BRs	Bioreactors
DIW	deionized water
HM	heavy metals
HRT	Hydraulic retention time
MCW	mine-contact water
Sb	antimony
Se	selenium
SeRB	selenate-reducing bacteria
Slurry	solids in water
Stibnite	antimony sulfide
TDS	total dissolved solids
TOC	total organic carbon
WRSA	Waste Rock Storage Area
YRC	YukonU Research Centre

1. Introduction

As the exploration and production phases of gold mining operations in the Yukon Territory increase, there is substantial emphasis being placed on the development of remediation technologies to treat mine-contact water (MCW) during closure and post-closure phases. The mining industry, as well as environmental protection agencies, specific departments within the government and First Nations, have been interested in the research and development of remediation methods to treat heavy metals such as selenium (Se), as well as metalloids such as antimony (Sb), and arsenic (As), all of which are commonly found in wastewaters of Yukon mines. Of particular interest to all stakeholders, is the development of passive or semi passive treatment technologies and bioremediation techniques, which make use of bacteria endemic to the Yukon Territory for the purpose of removing harmful concentrations of these contaminants. In addition to focusing on bioremediation, an emphasis on passive adaptations to these techniques has been highly sought after for its promise of reduced human intervention, and as a result, reduced costs.

Passive water treatment technologies such as bioreactors, which make use of relevant bacterial colonies to reduce various species of the identified metals, are often employed for chemical reductions of said metals when temperatures can support bacterial growth and efficiency. Additionally, through the respiratory pathways of specific anaerobic bacteria, waste products have been utilized within the bioreactor environment for adsorption and precipitation of metals as alternative removal processes.

This pilot scale study investigates the adaptation of Yukon native bacteria sampled from Eagle Gold mine site to seasonal freeze and thaw cycles and their subsequent capacity to remove As, Se and Sb from MCW.

This research project was conducted over the span of three years (7th of September 2019 to 13th of June 2022), and follows a laboratory scale study performed in 2015 at the Yukon Research Centre (Janin et al. 2015).

2. Literature Review

2.1. Selenium

Selenium (Se) exists in organic and inorganic forms in the environment. For the purpose of discussing its removal from mine-contact land and water, the inorganic speciation is most relevant. Se is found in four oxidation states: (2-) as organic selenides, (0) as elemental Se, (4+) which readily forms inorganic selenite (SeO_3^{2-}); and (6+) which readily forms inorganic selenate (SeO_4^{2}). Both selenite and selenate are highly soluble (Khamkhash 2017).

Selenium is found in low levels (1 mg/kg) in igneous and metamorphic rock, it can be as high as 100 mg/kg in sedimentary rock (MEND 10.1.1), and in surface waters found across Canada, concentrations of Se were found to range between <0.1 ug/L to 40 ug/L (Health Canada 1992). Typical pre-treatment concentrations of Se in mine wastewaters of a select number of mines in Canada ranged between 5 – 110 ug/L (MEND 10.1).

High concentrations of Se found in the environment typically have anthropogenic sources, such as coal mining and combustion; gold, silver, and nickel mining; metal smelting; municipal landfills; and agricultural irrigation. Mining, in particular, contributes to high concentrations of Se in the environment from leaching events from waste rock and tailings. Se makes up an important elemental component of the mineral matrix of metallic ore deposits which are sought after by the mine industry; specifically, sulfide-containing ores such as pyrite, sphalerite, chalcopyrite, among other sulfides. Ore processing involves methods such as froth flotation and leaching, which involves the chemical treatment of slurry (solids in water), that results in the dissolution of selenium in water. This dissolved Se, when discharged through tailings or wastewater streams, increases the risk of bioaccumulation in aquatic life. Se pollution from mining activity has been found in Yukon wildlife and fish populations (Lemly 2004; Khamkhash et al. 2017).

Although Se is typically observed at low concentrations in the environment, it easily bioaccumulates in the living ecosystem it is found in. There are two processes of Se bioaccumulation: bioconcentration and biomagnification. Bioconcentration is the direct uptake of Se from water or sediment across respiratory or epidermal surfaces, and primarily centres around

selenite and selenate, which are prevalent in aquatic systems. Biomagnification occurs via uptake and accumulation through the food chain, and involves organic selenium compounds, as well as inorganic species (Ogle et al. 1988).

Acute, or chronic Se toxicity, of inorganic Se species, to freshwater fish and invertebrates has been reported from concentrations ranging between 55 – 75 ug/L. One case study found concentrations of dissolved Se over 100 ug/L observed in Kesterson Reservoir, California, resulted in reproductive failure and birth defects in waterbird populations (Besser et al. 1993).

Selenium removal within Sulfate reducing bioreactor systems occurs through several biochemical reduction pathways. Some of these pathways are utilized by Sulfate Reducing Bacteria (SRB) species, thus explaining why there has been success in lowering Se concentrations in SRB bioreactors (Luo et al. 2008). A lesser studied bacterial species, and perhaps more relevant bacteria, is selenite and selenate-reducing bacteria (SeRB), which utilize oxidized Se species, such as selenite and selenate in their respiration, and in doing so, reduce selenite and selenate to elemental Se (0) and selenides (-2) (Sanchez-Castro et al. 2017; Hunter et al. 2007). Within SeRB bioreactors, successful removal of Se in the form of harmful selenite and selenate has been observed. One case showed a removal rate of 85% of selenate (via reduction to selenite) within a short retention time of 2.9 hours, and at a higher retention time of 95.2 hours, >99% of soluble Se was removed (Fujita et al. 2002).

2.2. Antimony

Antimony (Sb) exists in a variety of oxidation states (-3), (0), (3+) and (5+), oxidation states (3+) and (5+) are the most prevalent inorganic species in the natural environment, with Sb(OH)3 and $Sb(OH)_6$ being the dominant chemical species in aquatic environments (Filella et al. 2002). In soil solution, Sb is primarily present as pentavalent oxyanion, $Sb(OH)_6$ (Oorts et al. 2008). Critical natural sorbents of Sb in soil are Fe and Mn oxides (Mitsunobu et al. 2010). Typically, Sb is found at relatively low concentrations within ore deposits: 0.2-0.5 mg/kg in the earth's crust, less than 0.3-8.4 mg/kg in soils and less than 1 ug/L in unpolluted water (Liu 2010).

Antimony has had drastic growth in industrial use, through products, such as: flame retardants, alloys, pigments, and semiconductors. Often, the release of Sb into the environment is observed through mining and smelting activities (Okkenjaug et al. 2011). Sb can be found in high concentrations in soils from improperly disposed mine tailings and waste rock (Filella et al. 2002). Upon exposure to surface conditions, Sb associated with sulfide-rich ores, is quickly oxidized. However, the mobility of Sb depends on its oxidations state, available adsorption substrates, and composition of the aqueous matrix (Ritchie et al. 2013).

Although there is no biological function for Sb in either plants or animals, Sb is bioavailable to aquatic organisms living in contaminated habitats (Obiakor et al. 2018). Mobile forms of Sb found in plants growing in areas contaminated by mine wastewater, are usually relegated to the roots, lower shoots, and occasionally in old leaves and are not commonly found in plant segments above ground where animals graze from (Coughtrey et al. 1983; Hozhina et al. 2001). Acceptable levels of Sb in aquatic environments range around the world, from 3 ug/L in Australia, 5 ug/L in the EU, and up to 6 ug/L in the United States. Although bioconcentration and bioaccumulation are found in aquatic plants and in various concentrations across fish species, there is little evidence showing that Sb transfers to high trophic levels. On the contrary, there are diminishing effects on concentrations moving from lower to higher trophic levels (Obiakor et al. 2018).

Primary passive removal methods for Sb from mine wastewater are either via adsorption onto iron oxyhydroxides, or via precipitation as antimony sulfide (stibnite) in a sulfate-reducing bioreactor. Typically, adsorption techniques have high removal rates at first, with quickly diminishing removal rates over time as adsorbents reach their capacity to adsorb contaminants. However, sulfate-reducing bioreactors, particularly ones with hydraulic retention times of 24+ hours, have shown to be increasingly successful over time in reducing Sb. This is due to the cultivation of sulfate-reducing bacteria colonies within the bioreactors, as their metabolic waste product is typically hydrogen sulfide, which reacts with metal ions to produce the stibnite precipitate (Trumm et al. 2015). Various removal rates of Sb in sulfate-reducing bacteria bioreactors have been observed: 98.8 and 99.4% over 2-14 days (Liu et al. 2018), 93% over an 11-day period (Zhang et al. 2016), and 99.2% over 7 days (Wang et al. 2013).

2.3. Arsenic

Arsenic (As) occurs in all geologic materials, however, the major natural source of arsenic to the environment is volcanoes. However, As in waterways is usually attributed to anthropogenic sources, such as fossil fuels, mining wastes, agricultural use, or irrigation practices (Korte and Fernando 2009). As found in the environment, exists in four oxidations states: arsine (-3), elemental arsenic (0), arenite (+3), and arsenate (+5). In oxic waters, As5+ is thermodynamically stable state, while As3+ is prevalent in reduced redox environments. As (III) is more mobile and toxic, in comparison to As (V). Although As (III) can also become immobilized in the presence of sulfide (Bissen and Frimmel 2003; Stauder et al. 2005).

As concentrations in rain derived from unpolluted oceanic air masses average 0.019 ug/L, and rain from terrestrial air masses average 0.46 ug/L. Groundwaters can range vastly in As concentrations, between 0.01 to 800 ug/L. Although, generally, groundwaters contain less than 0.001 ug/L (Andreae 1980; Boyle and Jonasson 1973).

As minerals often accompany gold and copper ores, since they all share the same chalophillic behaviour, and beneficiation of these ores can release As via process waters into the environment (Bissen and Frimmel 2003; Matschullat 2000). Due to the acidic conditions created by acid mine drainage (AMD), arsenic sulfidic ore such as arsenopyrite (FeAsS) leaches arsenic from gold heap leaches (Roussel et al., 2000). However, metal leaching of As from arsenic minerals at neutral pH due to oxidation can occur in heap leach waste (Mend 10.1).

Biomagnification of As across various trophic levels of aquatic organisms is not consistent, and generally, concentrations decrease through the progression to higher trophic levels. However, bioaccumulation is obvious in aquatic food chains. Aquatic organisms accumulate arsenic mainly as inorganic forms, and some of the organisms such as phytoplankton, bacteria, etc. transform them into methylated and organic forms (Rahman et al. 2012).

In humans, inorganic forms of As are converted to organic monomethylated and demethylated metabolites, which have a cytotoxic and genotoxic effect, as well as become inhibitors of pivotal enzymatic functions. As methylation of inorganic As has long been considered a pathway for the detoxification of the metalloid, it is now understood, that this process has more insidious

consequences in the body (Thomas et al. 2001). As is understood to be a carcinogen. Cancer of the skin, lungs, urinary bladders, kidney, and other sites, has been observed in people with long-term exposure to inorganic As. The genotoxic effect of As, in addition to oxidative stress, growth factors expression, and loss of DNA repairing mechanisms are proposed to be the mechanisms by which As promotes carcinogenesis within the human body (Khairul et al. 2017). Much like Sb, the removal mechanism for arsenic in SRB bioreactors is through precipitation of As species with sulfide by-products of SRB colonies. However, the relationship between As species and sulphides is slightly more complex in its chemistry, compared to Sb. Typically, As precipitates with sulphides to form arsenic sulphide As_2S_3, thus decreasing As concentrations. However, as sulphide concentrations within a bioreactor rise, the re-dissolution of the newly formed arsenic sulphides form thioarsenite complexes, and therefore increase arsenic concentrations. To add to this complexity, a decrease in As concentration observed in SRB bioreactors can be attributed to the presence of various metal sulphides, which are known to be strong arsenic scavengers that can accommodate significant amounts of arsenic in its crystal lattice (Castro et al. 1999; Webster 1990). In spite of this sensitive balance between As species and sulfides, generally, As removal rates in SRB bioreactors range between 60 – 96% (Jong and Parry 2003; Simonton et al. 2000; Uhrie et al. 1996).

3. Material and Method

3.1. Experimental Setup

Four 200 L pilot-scale BRs were installed August 7th and 8th, 2019, at the Eagle Gold mine in central Yukon Territory, Canada. The BRs were installed in duplicates; two (BR1 and BR1b) were installed in the YukonU Research Centre (YRC) shed, and another set of duplicates (BR2 and BR2b) were installed outside of the shed. The BRs in the shed were heated to maintain a minimum temperature of 5°C over winter and left to fluctuate with outside temperatures when over 5°C, while the two outside of the shed were exposed to freezing, to evaluate the impact of freeze and thaw seasonal cycles on the bacterial population. The shed, established at the camp by Victoria

Gold, had the following dimensions: 8’ (W) × 11’ (H) × 12’ (D) (figure 1). This set up, and more specifically, the expected bacterial population contrast that should be measured in the BRs located outside the shed versus within the shed, will help to indicate the physiological adaptation of the community to cold temperatures on site (Nielsen et al. 2018).

BRs inside the shed

BRs outside the shed

YRC shed

Figure 1: BR1 and 1b(a); BR2 and 2b(b) and YRC Shed(c).

Each BR was comprised of an open-top 55-gallon polyethylene drum, covered with a lid, and a steel lever lock (Uline, Milton, ON, Canada). The mine-contact water (MCW) and carbon source were fed through an inlet pipe installed near the bottom of the BRs. The MCW flowed from the bottom to the top to push oxygen out of the system and ensure anoxic conditions. The outflow went to each collector drum through the outlet pipes which were installed on the lids of each BR. Bulkhead fittings (Green Leaf, Fontanet, IN, USA) and reducing bushings (Cole Parmer Canada, Montreal, QC, Canada) were used to connect the tubing (C-Flex L/S 16 Tubing 50 A; Cole Parmer Canada, Montreal, QC, Canada) to the BRs and collector drums. Two collector drums inside of the shed remained open, while the other two collector drums outside of the shed were covered with lids and steel lever locks to prevent leaves and dust from entering the collectors. Digi-Sense temperature probes were installed on the lid of each BR and sealed with silicone to keep the BRs anaerobic. 30-psi pressure relief valves (Apollo Valve, Mattews, NC, USA) were also installed on the lid to prevent pressure higher than 30 psi in the BRs (figure 2).

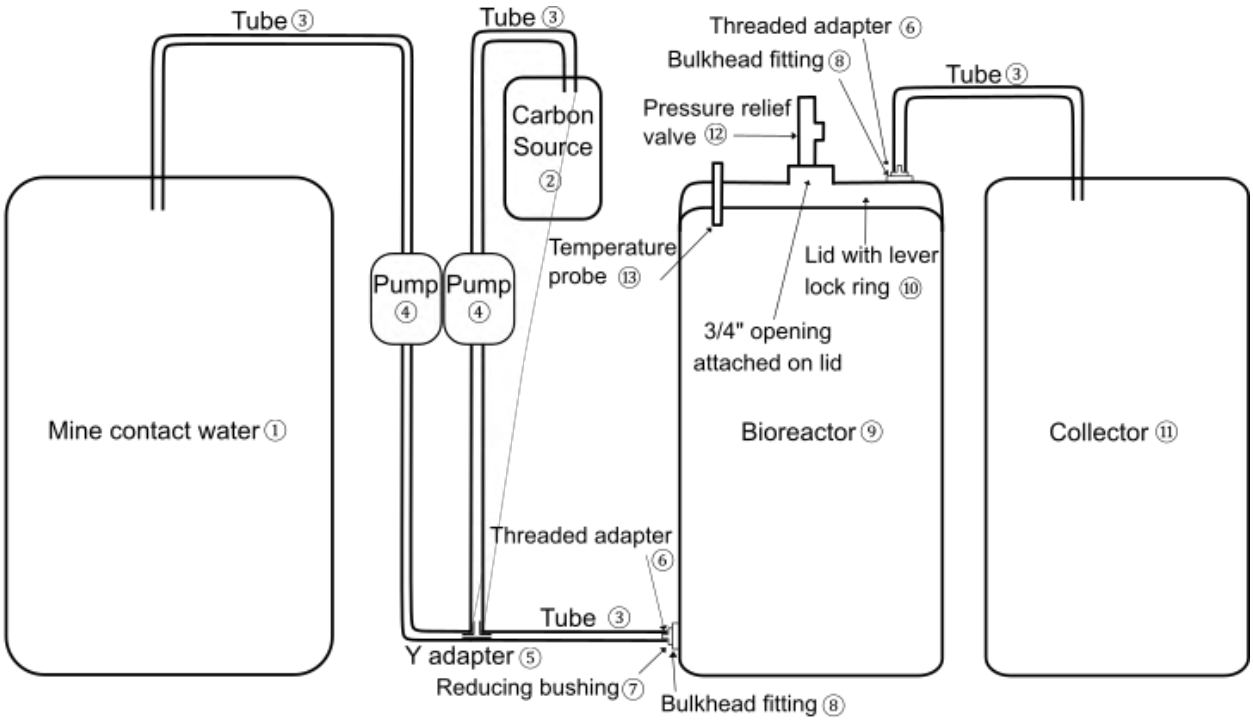

Number	Name	Number	Name	Number	Name
①	Intermediate bulk container	⑥	1/8" NPT - 1/8" ID nylon threaded adapter	⑪	55 gallon open head polyethylene drum
②	10L glass with magnetic stirrer	⑦	3/4" NPT - 1/8" ID nylon reducing bushing	⑫	30-psi pressure relief valve
③	Masterflex L/S 16 Tubing	⑧	2" NPT - 3/4" NPT nylon bulkhead fitting	⑬	Digi-sense replacement temperature probe
④	Masterflex peristaltic pump	⑨	55 gallon open head polyethylene drum		
⑤	1/8" ID Y adapter	⑩	Polyethylene lid with steel lever lock ring		

Figure 2: Experiment design for this study.

Each BR was filled with 20% v/v wood chips (local Yukon white spruce) and 20% v/v inoculum. The inoculum was a mixture of samples from two different wetlands in the same drainage of and close to Eagle Gold Mine, locations 0459110E 7100937N and 0458249E 7099695N, respectively (Table 1). A previous experiment revealed that the addition of spruce chips supported biofilm growth (Janin et al. 2015), therefore, locally sourced, shredded spruce chips, ranging from 1-2 inch pieces, were used for this experiment. The wood chips and inoculum were mixed thoroughly in the BRs, and the remaining 170L was filled with MCW, measured on site, by 20L buckets.

Table 1: Inoculum site coordinates and location description

	UTM Coordinates	Location Description
Inoculum Site 1	Zone 8W 0459110E 7100937N	Eagle Creek diversion / W61
Inoculum Site 2	Zone 8W 0458249E 7099695N	20 m upstream of W45

The MCW was pumped from the Platinum Gulch Waste Rock Storage Area (WRSA) and transported to the YRC shed by Victoria Gold environmental staff biweekly. The three potential locations from the WRSA to collect the MCW were: the exit of the pipe near the treatment pond, the entrance of the pipe at Platinum Gulch Waste Rock Pile, and the pond above ditch A (figure 3). During winter, the WRSA did not produce any water and MCW from the treatment pound or Low-level outlet (LLO) was used to fill the water tank. The MCW tank was emptied before refilled up biweekly to reflect Platinum Gulch WRSA water.

Figure 3: MCW sampling locations: (a) pipe exit near the treatment pond; (b) the pipe entrance at the Platinum Gulch Waste Rock pile, and (c)the pond above ditch A.

Hydraulic retention time (HRT) of 2 weeks was chosen following a previous lab scale experiment with similar parameters (Janin et al. 2015). The constant MCW flow rate, 10.63 mL/min, was calculated based on the HRT. The flow rate was controlled by a peristaltic pump (Masterflex L/S Standard Digital Drives; Cole Parmer Canada, Montreal, QC, Canada) with a Masterflex L/S 6-channel, 6-roller cartridge pump head (Cole Parmer Canada, Montreal, QC, Canada).

Following the studies performed by Nielsen et al. (2018), molasses was chosen as the carbon source (Crosby's 100% Natural Fancy Molasses; Crosby Molasses Company Limited, St. John, NB, Canada). The molasses solution was prepared biweekly, on site, and was continuously stirred by via a magnetic stirrer (equipment info needed). The amount of molasses in the molasses solution was calculated based on the sulfate concentration that was analyzed by ALS on a weekly basis (Eq. 1). In order to calculate the amount of carbon needed to feed the BRs, a minimum of 100mg/L of sulfate was considered, even if results from ALS analysis showed lower sulfate concentrations.

Equation 1: $SO_4{}^{-2}{}_{(aq)} + 2C(organic)_{(aq)} + 2H_2O_{(aq)} \xrightarrow{SRB} H_2S_{(aq)} + 2HCO_3{}^-$

The peristaltic pump's (Masterflex L/S Precision Variable-Speed Console Drives; Cole Parmer Canada, Montreal, QC, Canada) flow rate was set to 6 mL/min and was set to pump automatically via a timer (equipment info needed) for 22 min/day to have the exact amount of carbon required pumped into the BRs.

After 2 years of maintenance and monitoring, it has been realized that some Arsenic was being leached out of the bioreactors. While investigating the causes of the leaching phenomenon (discussed in section 4.8), Victoria Gold asked the Northern Mine Remediation team to investigate technologies that could remove As from BRs' effluent.

In July 2021, two cylindrical columns (figure 4) made of 1.1 cm thick Plexiglas™ were used for this experiment. The internal diameter of these columns was 6.4 cm, and the length was 63 cm. Each column was sealed closed at the bottom by bolting a Plexiglas™ plate to it with the same external diameter. Between the column and end plate, a rubber gasket was used to ensure an air-tight seal was achieved. Each end plate was fitted with an outlet port with ~ 1 mm opening hole and sealed additionally with epoxy. L/S Masterflex 16 ID tubing (Cole-Parmer Canada Company, Montreal QC) was attached to the outlet port. The flow from BRs to the columns was going from the bottom to the top and was then collected in an outlet.

Figure 4: Columns C1 and C1b installed in series of BR1 and BR1b in the onsite research shed.

The columns C1 and C1b, installed in series of respectively BR1 and BR1b, were filled up with a certain volume of Zero Valent Iron (ZVI). In order to assess the impact of ZVI for As removal, C1 was filled up with 100% volume of ZVI while C1b was filled up with 50% volume of ZVI.

3.2. BR Monitoring and Chemical Analysis

The data and samples were collected by the Victoria Gold environmental staff on a weekly basis. The samples from effluent drums were collected after stirring the contents. When performed by YukonU staff and researchers, conductivity and pH of MCW tank and effluent drums were recorded. The temperature of the BRs and MCW tank was also recorded. Conductivity and pH measurements were performed using a pHmeter (PCD650 m; Oakton, Australia) equipped with a double junction Ag/AgCl electrode (Cole Parmer Canada, Montreal, QC, Canada). Calibration of the pHmeter was performed using a certified solution (ORP Standard; Fisher Scientific, Montreal, QC, Canada). The meter was rinsed with deionized water (DIW) between each sample. Samples for total organic carbon (TOC) were preserved with sulfuric acid (2%, v/v). Samples for heavy metals (HM) were preserved with nitric acid (2%, v/v). When measurements were done by Victoria Gold staff, a YSI PRO DSS was used.

Table 2: Parameters followed during experiment.

Weekly sampled:	**Monthly sampled:**
Volumes of treated water outlets	Bacterial sample
Temperatures (Outside, inside shed, inside BRs)	ORP
Conductivity	
Heavy Metals	
Sulfate	

Samples were sent an on weekly basis to ALS, Whitehorse. Methodology used for each parameter is described in ALS certificate of Analysis provided in Annex 2.

3.3. As leaching experiment

High As concentration were detected in the BRs' effluent over the 1-year experiment (see section 4.8) that might be sourced to the inoculum. To investigate the possibility that inoculum could be the source, a set of leaching experiments where designed.

An acid-based extraction followed by an ion-exchange resin experiment was performed at the YukonU Research Center on the inoculum to extract and investigate the speciation of As (As(III) versus As(V)). Inoculum from two different sites of the Eagle Gold mine were sampled: site 1 and its duplicate 1b, and site 2 and its duplicate 2b. Samples were collected in buckets. In each bucket (site 1, site 1b, site 2 and site 2b) five sub-samples were taken: four evenly spaced on the border of the bucket and one in the center. Sub-samples were then mixed manually before being used in the leaching test.

Volume baffled bottom flasks (500 mL) were filled with about 75 mL of inoculum and 300 mL of distilled water to achieve 20% v/v inoculums ratio present in BRs. Resulting mixtures were agitated on an agitation table and sampled after 24 hours, 14 days and 31 days after mixing. During each sampling, mixtures were removed from agitation table and filtered using 45 µm disk filters. For As total metal analysis (As TM) 20 mL of filtered sample were collected in 50 mL sample bottle using acid-washed 30 mL Luer lock syringe and acidified using 1.0 mL of 18% HNO_3. To measure the concentration in As(III), 30 mL of unacidified sample was passed slowly using a flow rate of ~ 4 mL/min through acid-washed, pre-moistened with a few mL ultra-pure H_2O Supelco LC-SAX tube and then, acidified with 1.5 mL of 18% HNO_3. The weight of sampled bottles was recorded before and after the filtration. To access to As(V) concentration, 10 mL of 1M (6%) HNO_3 was passed through the previously used LC-SAX tube at a flow rate of approx. 4 mL/min using syringe except for test 3 (after 31 days of mixing) where 30mL of acid was used to maintain equal volumes. The process was repeated for the four mixtures from the two sites and DIW (reference/ standard) and sent to ALS, Whitehorse for As concentration detection.

3.4. Biological Sample Collection

A passive sampling method was used to collect the microorganisms growing inside the BRs. The microorganisms sampled were assumed to be representative of the bacterial communities within the BRs, originating from the inoculum used for treatment within the BRs. Sampling bags were made with light cotton material used for flour sacks and filled with silica sand to keep the bags submerged in the BRs. Twelve sampling bags were suspended into the middle of each BR with fishing line through a hole on each lid at the beginning of the experiment, the hole was then sealed with silicon. Sampling bags were collected monthly from each BR by breaking the silicon seal, retrieving a sampling bag, replacing it with another, and sealing the hole again with silicone.

DNA characterization will be completed on each sampling bag for identification of bacterial species once the pilot experiment is completed (to be determined). An updated methodology will be added at this point. Sampling bags were frozen by liquid nitrogen in a thermo flask (container 2122 Thermo scientific) immediately after collection from the BRs and transported from the field to the laboratory for storage at -86°C until DNA extraction could occur. **The genomic characterization will be part of a peer reviewed publication in 2023 and, therefore, is not discussed in this report.**

4. Results and discussion

For all the figures presented below, it is important to note that between October 11, 2019, and May 12, 2020, October 16, 2020, and May 23, 2021, and September 23, 2021, and June 13, 2022, both duplicates of BR2 (the BRs located outside), were considered frozen and measurements could no longer be taken. Note that freezing and thawing periods likely correspond to a series of small freeze-thaw events, rather than one freeze event in the fall and one thaw event in the spring. However, since temperature was measured on a weekly rather than continuous basis, we were not able to accurately indicate when specific freeze or thaw events took place. Thus, no data points are plotted during these periods in the following charts.

4.1. pH

The pH of MCW, average BR1, and average BR2 was sampled at least twice a month over the three-year period. Throughout the span of the experiment, the pH remained around neutrality, verging towards basic specifically for MCW (figure 5). The pH of MCW appeared to be consistent over the length of the experiment and was comprised between 7.2, sampled on October 4, 2019, and 9.3, sampled on September 12, 2019.

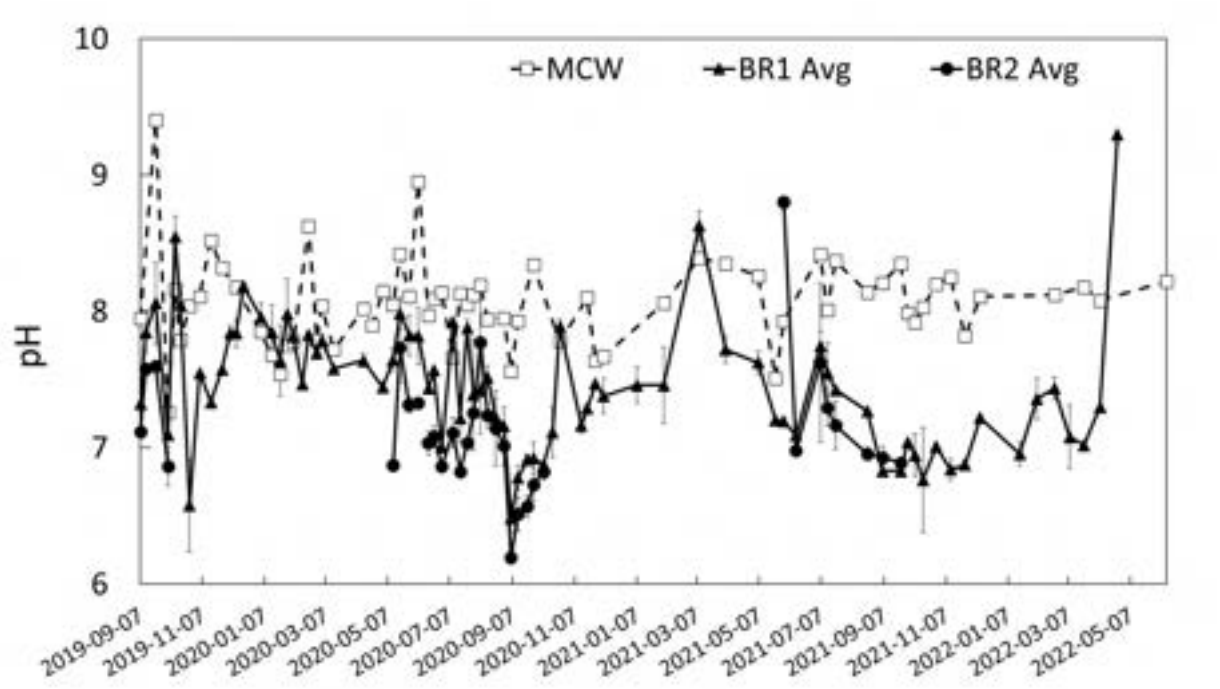

Figure 5: pH of mine-contact water (MCW, empty square and dashed line), average BR1 (BR1 Avg, black triangle and full line) and average BR2 (BR2 Avg, black circle and full line) function of time.

The general trend of average pH for BR1 effluent appeared to parallel the pH from MCW, with slightly more acidic values, and reached the most basic pH of 9.2±0.0 on April 24, 2022, and the most acidic pH of 6.4±0.1 on September 5, 2020.

During the non-freezing period in the study's first year (September 7 to October 4, 2019), the BR2 average pH ranged from 6.7 to 7.5 and closely mirrored BR1 average pH, which ranged between

7.0 and 7.9 during the same period. BR2 tended towards slightly more acidic values but were consistently within 0.2 to 0.5 pH units during this time. The pH values for BR2 average were comprised between 6.1±0.0 on September 5, 2020, and 8.7±0.0 on May 31, 2021. Throughout the experiment, BR2 average pH values consistently saw an increase by one pH unit from values before freezing in the fall to pH values obtained after seasonal thaw in the spring.

4.2. Conductivity

In many cases, conductivity was linked directly to the total dissolved solids (TDS) and provided a good analogue for the concentration of dissolved salts within the MCW and BRs. Figure 6 presents conductivity measurements in MCW, BR1 average and BR2 average over the 3-year experiment.

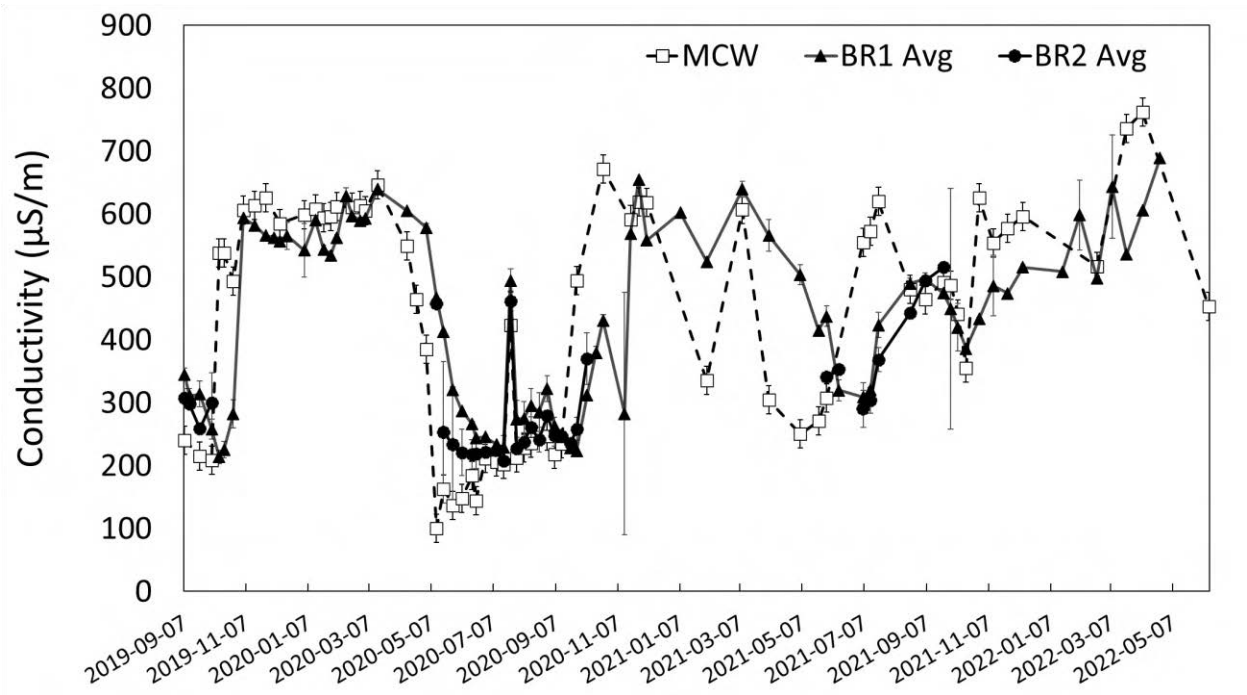

Figure 6: Conductivity, in µS/m, of mine-contact water (MCW, empty square and dashed line), average BR1 (BR1 Avg, black triangle and full line) and average BR2 (BR2 Avg, black cycle and full line) function of time.

The conductivity of MCW displayed its lowest annual values (generally between 200 and 300 µS/m) during the summer months each year stabilizing in the range of 600-700 µS/m for fall

and winter, before plummeting back to summer values in early spring. This seasonal cycle held for the duration of the experiment, although winter values showed increasing variability throughout the course of the study in contrast with the relatively stable values of winter 2019/2020. This general pattern persisted throughout the duration of the study, with a slight upward trend in MCW conductivity values. MCW conductivity showed a greater range of values than either of the BR tanks, with the highest value of 762.0 μS/m on April 7, 2022, and the lowest values of 100.1 μS/m on May 12, 2020.

Regarding the BRs, the conductivity measured in both BRs seemed to globally mirror the conductivity measured in the MCW. For instance, from January 3 to March 15, 2020, MCW conductivity ranged from 594 to 646 μS/m, with BR1 values between 535 and 649 μS/m during the same time period. Conductivity values between MCW and BRs again converged from July 10 to September 12, 2020, when MCW values ranged from 202 to 423 μS/m, BR1 from 229 to 495 μS/m and BR2 from 207 to 461 μS/m.

For BR1 average, the conductivity generally demonstrated slightly less amplitude than MCW values, with summer lows generally around 300 μS/m and winter highs closer to 500 μS/m. The degree of variation outside of the general seasonal pattern increased throughout the study, with the same upward trend in all values as MCW during the final year of the study. Seasonal increases and decreases were generally observed for BR1 average with a 1-month delay in response to changes in MCW conductivity. This delay period between MCW and BR1 values gradually lengthened throughout the experiment, eventually becoming closer to a 2-month delay by the end of the study.

Conductivity for BR2 average followed the same trend as BR1 average before the first freezing event. After spring thaw, even though the trend for BR2 average was like BR1 average, the values detected were a bit lower than the one measured for BR1 average, with values lower by around 10 μS/m in BR2 average. Data from the second thawing period continued this general trend with BR2 values averaging approximately 20 μS/m less than average BR1 values. Despite the delay between trends in MCW and BR averages, there were several spikes (both positive and negative) which were detected simultaneously for MCW, BR1 average and BR2 averages throughout the study. The first spike occurred on March 15, 2020, with a MCW value of 646 μS/m and similar value of

640 μS/m in BR1 (BR2 was frozen at this time). Another simultaneous high point across MCW and BR1 occurred on March 9, 2021, with 607 μS/m for MCW and 640 μS/m in BR1.

4.3. Calcium

Throughout the experiment, MCW values for Ca, shown in figure 7, generally fell between 60 and 70 mg/L during freezing periods with an average of 65.9±21.2 mg/L and typical values between 30 and 50 mg/L during thawing periods with an average of 44.5±17.1 mg/L. It can be noted that a sudden decrease in Ca concentration was observed in January 2020. This decrease is due to the freezing of the MCW source in mid-January given extreme cold conditions. The seasonal fluctuation of Ca in MCW was suggestive of dissolution/concentration processes associated with freeze/thaw cycles.

MCW Ca concentration followed trends based on seasonality, which could be explained by seasonal dilution during the "thawing" period (corresponding to late spring, summer and fall in the Yukon), resulted in lower values for Ca concentration. Conversely, during the "freezing" period (late fall, winter, and early spring), the amount of free-flowing surface water was lower and thus, the concentration in TDS increased, possibly favoring the corresponding rise in calcium concentration.

BR1 and BR2 (when thawed), followed similar trends and generally paralleled the concentration behavior of MCW. Similar to what we observed for the conductivity, there was a small offset between the MCW and the BRs' signal, but contrary to what was observed for the conductivity signal, the offset was varied either anterior or posterior to the Ca concentration in MCW. Continuing the similarities with conductivity was the growth in temporal offset or delay between MCW and BR values, which lengthened throughout the second and third years of the study. Both BR tanks experienced a drastic spike near the end of the experiment on March 31, 2022, with a BR1 average of 225 mg/L and the BR2 average reaching 254 mg/L on the same day. These values are nearly threes time greater than any of the previous maximums from the 3-year experiment. Ca concentrations demonstrated even higher values in both BR averages on the following measurement, April 21, 2022, before the termination of the experiment, with BR1 average of 363

mg/L and BR2 average of 338 mg/L on that day. The final data point showed a descent in Ca concentration in BR1 average from this spike before the end of the experiment, with an average concentration of 77.5 mg/L on April 24, 2022, while there was no data available for BR2 on this day. The origin of this Ca spike event is difficult to identify since the Ca concentration in MCW are missing.

The high similarity between BRs' effluents concentration and MCW was a strong indication that Ca is not removed by the BRs, thereby resulting in negligible precipitation of Ca-based minerals (gypsum or ettringite) in the BRs, independently of the BRs' temperature.

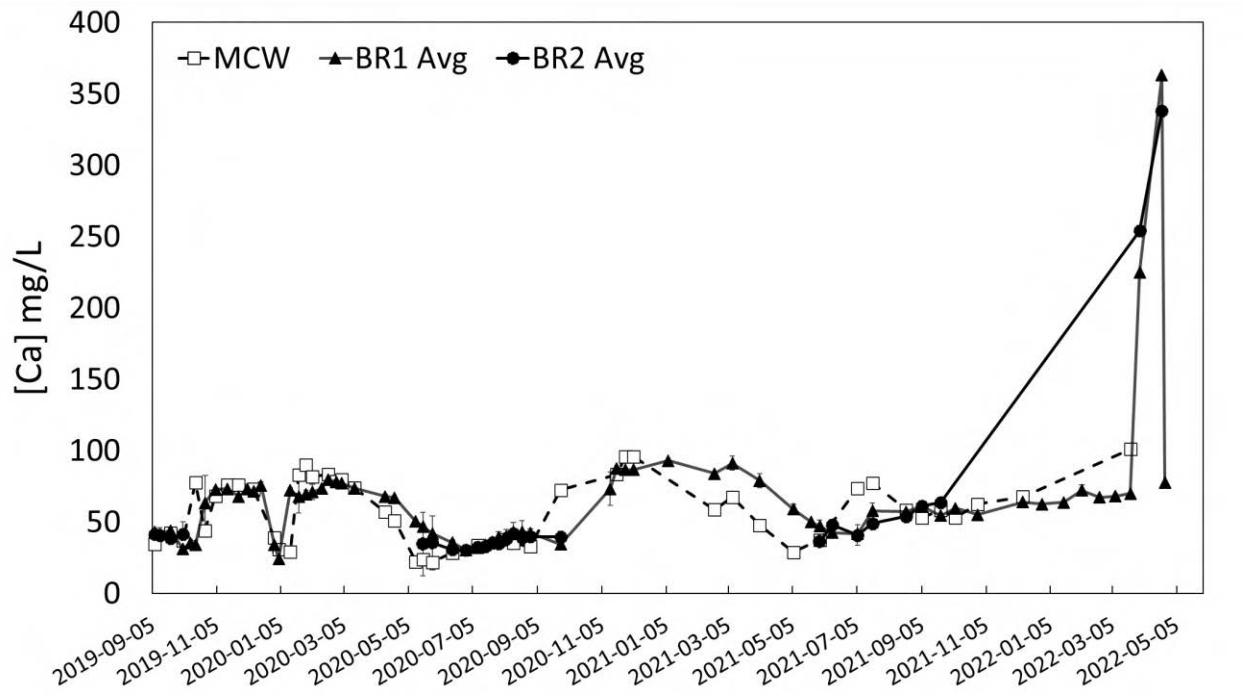

Figure 7: Calcium in mg/L, of mine-contact water (MCW, empty square and dashed line), average BR1 (BR1 Avg, black triangle and full line) and average BR2 (BR2 Avg, black cycle and full line) function of time.

4.4. Iron

Throughout the experiment, iron concentration (shown in figure 8) in MCW ranged from 0.03 to 36.0 mg/L, with consistently low values occurring during winter month in the first two years of the study. Iron concentrations from January to March 2020 averaged to 0.17±0.14 mg/L, with

similarly low concentrations averaging below 0.5 mg/L during the same month of the following year. Winter 2022 had few data points, making it difficult to identify trends towards the end of the experiment. Summer months typically saw higher concentrations and a greater degree of fluctuation between measurements, with an average of 9.52±12.4 mg/L from May through August, 2020, and an average of 5.72±4.48 mg/L during the same months of summer 2021. MCW iron concentrations averaged to 4.60±8.63 mg/L throughout the duration of the experiment.

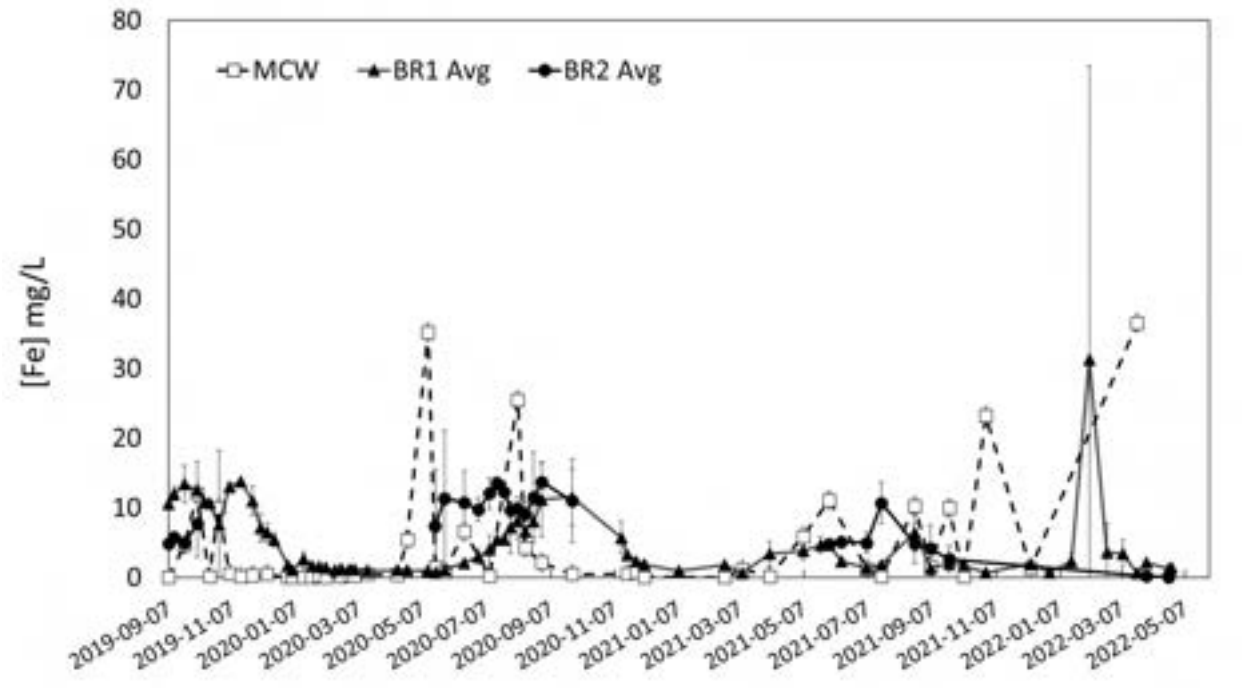

Figure 8. Iron in mg/L, of mine-contact water (MCW, empty square and dashed line), average BR1 (BR1 Avg, black triangle and full line) and average BR2 (BR2 Avg, black cycle and full line) function of time.

Iron concentrations in BR1 initially followed appeared to follow similar trends to MCW, though often with a delay of several months. For instance, while MCW peaked for 2020 on May 2, 2020, with a value of 35.2 mg/L, BR1 followed the trend of low values throughout the winter and peaked later on September 27, 2020, with an iron concentration of 11.5 mg/L. BR1 average iron concentrations ranged from 0.63 mg/L on March 22, 2022, to 31.3 mg/L on February 4, 2022. BR1 iron concentration showed a similar average to MCW and less variation over the duration of the study, with an average of 4.74±5.03 mg/L.

BR2 average concentrations fell within a similar range to BR1, with values ranging from 0.08±0 mg/L on April 21, 2022, to 13.5±0.99 mg/L on July 17, 2022. Although BR2 average values were often higher by 5 – 10 mg/L than those in BR1 throughout 2020 and 2021, they generally followed

similar seasonal trends and showed comparable spikes. For instance, during the thaw period in 2020, BR2 average reached its highest concentration of 13.5±0.99 mg/L, while BR1 average's highest concentration during that time frame was 11.5±4.04 mg/L. BR2 average also demonstrated the greatest consistency throughout the experiment and the lowest standard deviation among MCW and BR1 values, with an average of 7.78±3.84 mg/L. As well, BR2 average spikes in iron concentration were less than half of the highest concentration values for both MCW and BR2.

4.5. Sulfate

Sulfate concentrations in MCW and in BRs' effluent and subsequent calculated sulfate removal can be used to estimate bacterial activity. Indeed, sulfate removal, when not attributed to gypsum or ettringite precipitation, was used as an indicator of SRB's activity, reducing sulfates into sulfides. Figure 9 presents the evolution of sulfate concentration in MCW and the average sulfate concentration in BRs'effluent.

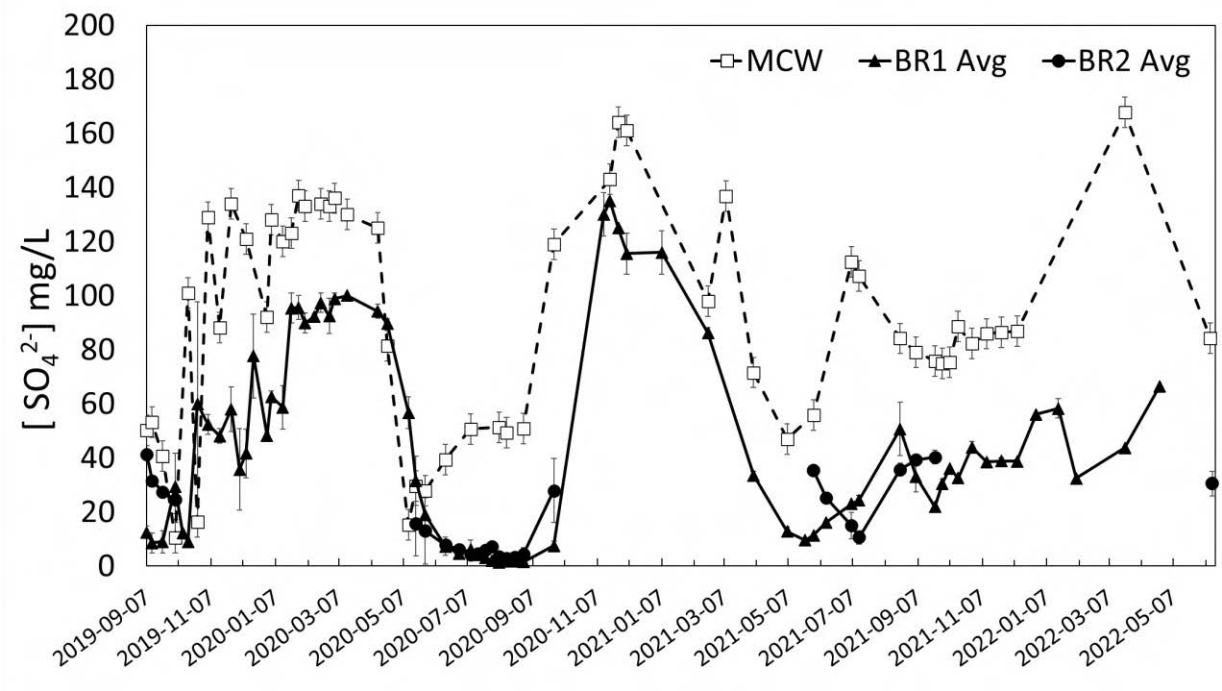

Figure 9: Sulfate concentration in mg/L in mine-contact water (MCW, empty square and dashed line), average BR1 (BR1 Avg, black triangle and full line) and average BR2 (BR2 Avg, black circle and full line) function of time.

Sulfate concentration of MCW followed a similar seasonal pattern to both conductivity and Ca, with relatively high values during the freezing months and lower values throughout the thawing months. This pattern continued until deviation occurred in winter 2021/2022, as values stabilized at around half of their normal winter peaks. Freezing values for sulfate in MCW generally ranged between 90 and 140 mg/L with an average of 107±36.5 mg/L, while thawing values typically ranged between 20 and 70 mg/L and averaged 60.4±29.2 mg/L. Variations in sulfate concentration in the MCW during the study's first year may be partly linked to change in water source sampling. Indeed, until November 11, 2019, water source was provided from Ditch A location. On November 11, 2019, the MCW location recorded is LLO through to May 2, 2020. On May 12, 2020, MCW was sampled from Ditch A sump and was sampled from here through to the end of our study.

In addition, the evolution in sulfate concentration in MCW also appeared to be dependent on seasonality, with higher concentration during the "freezing" season (concentration process), and lower concentration during the "thawing" period (dilution process).

Globally, the concentration in sulfate in the BRs mirrored the evolution and the seasonality of the MCW sulfate concentration. However, the concentration detected in the BRs effluent was almost always inferior to the one detected in the MCW. Similar, to our observations for conductivity measurement, an offset in decreasing or increasing events were observed between MCW and BRs, which gradually lengthened throughout the study.

Regarding specifically BR2: before the first freezing period (2019), the average concentration in BR2 effluent was slightly higher than the BR1 average apart from the last data point measured before the freeze event on October 4, 2019 with BR1 average 29.4±12.3 mg/L and BR2 average 24.6±5.25 mg/L. The average concentration in sulfate for BR2 in May 2020, i.e., when the BRs were thawed, was lower than the concentration detected in BR1 average, ranging from 18.9 to 56.8 mg/L for BR1 average and 13.0 to 15.6 mg/L for BR2 average during the same time period. The two BRs presented similar concentrations during the spring and summer 2020 until BR2 increased in sulfate concentration on the 27th of September 2020, which was the last data point collected before the tank froze for the season. Sulfate values in BR1 average ranged from 1.46±0.08 mg/L on August 6, 2020, to 135±0.00 mg/L on November 19, 2020, with an average value of 46.7±37.1 mg/L over the course of the experiment. During the following thaw cycle in spring 2021, BR2 averages were slightly higher than average concentrations in BR1, though generally within 10 to

20 mg/L, and consistently lower than sulfate concentrations in MCW. The BRs only had one data point for the thaw cycle in 2022 before the study's end, so it was not possible to identify trends in the final thaw cycle.

As stated before, even though the trend in concentration evolution was similar before MCW and BRs, sulfate concentration in BR1 and BR2's effluent was consistently lower than in MCW. Figure 10 presents the percentage of sulfate removal in BR1 average and BR2 average.

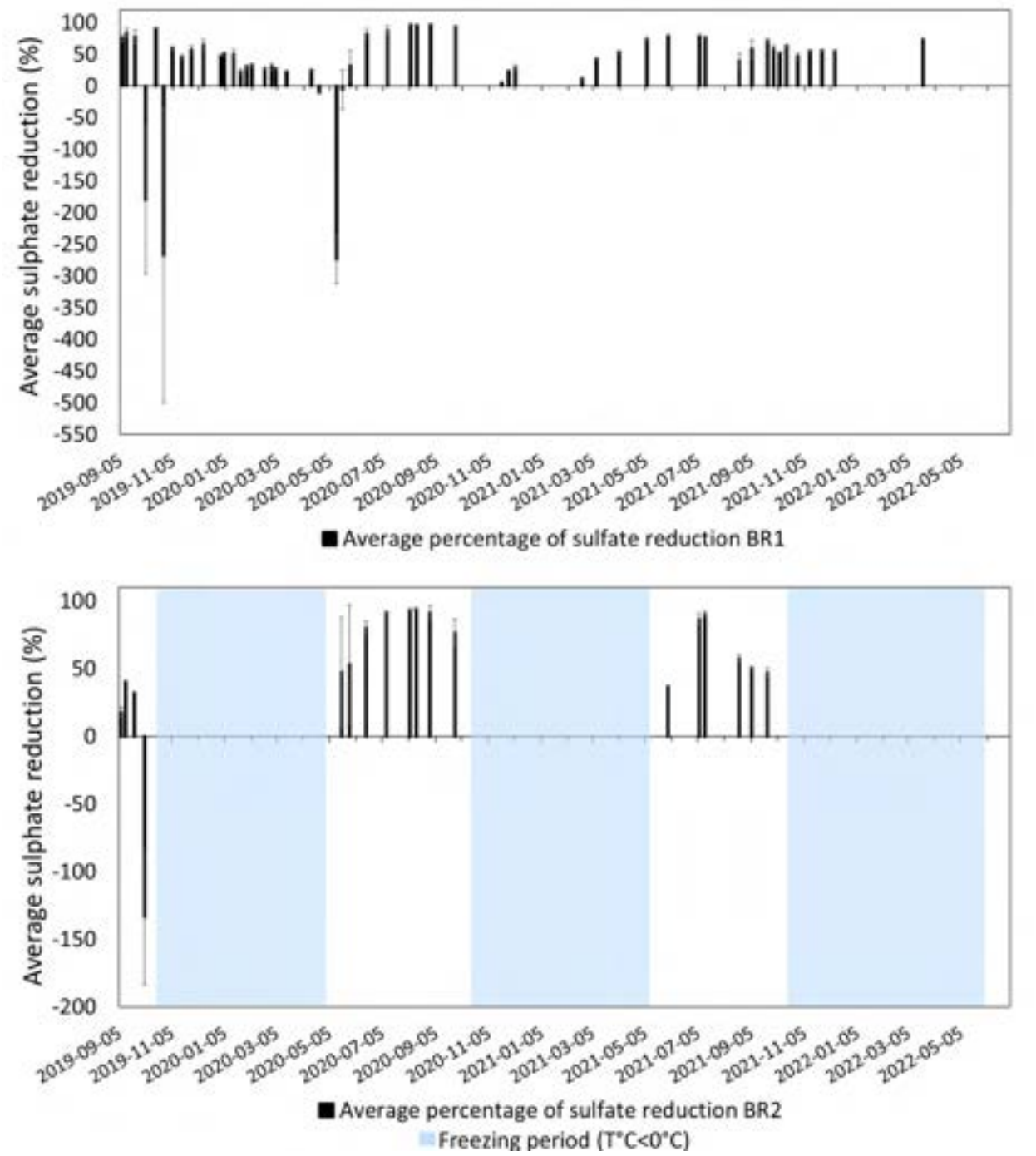

Figure 10: Percentage of sulfate removal from BR1 average (top) and BR2 average (bottom) function of time. The freezing periods are represented in blue in BR2 chart.

The BRs generally showed positive sulfate reduction rates, indicating an important capacity for sulfate removal. The positive percentage of removal is usually linked to either sulfate removal by co-precipitation with Ca or sulfate removal by sulfate-reducing bacteria (SRB). Indeed, high Ca

concentrations may lead to gypsum precipitation ($CaSO_4$) or ettringite precipitation ($Ca_6Al_2(SO_4)_3(OH)_{12}\cdot 26H_2O$) when in the presence of sulfate in solution (Tolonen et al. 2015). We observed previously (4.3) that Ca concentration in BRs is similar to the one detected in the MCW, which indicated no consummation of Ca by the bioreactor. The removal of sulfate by BRs is thus, probably due to the microbial activity of SRB bacteria in the BRs. In addition, ORP measurements (not shown) were taken monthly and ranged between -160.8mV (winter) and -378.2 mV (summer). Optimal ORP values for SRB to catabolize sulfates and release sulfides is in the range of -100 to -300mV (Gloyna, 1971; Gibert et al. 2002; Harerimana et al. 2010). Hence decreased ORP results observed in summer may be attributed to an increase in SRB activity.

The percentage of sulfate removal is negative four times for BR1 average and one time for BR2 average. Negative sulfate removal occurred when a small offset was observed between the evolution of the MCW and the BRs. Thus, it can likely be attributed to a lag-time due to the operation of the BRs, where all the sulfate was not consumed fast enough between two sampling events. Indeed, in the four times we observed those negative sulfate removal values, the previous sulfate concentrations were quite high and the corresponding MCW values were at the lowest. Thus, we do not consider those negative values as an indicator that the BRs were not working well, these negative events in the first year of the study may simply indicate that BRs require some initial start-up time before reaching maximal efficiency.

Figure 11 presents only the positive percentage of sulfate removal plotted with the temperatures function of time. Not surprisingly, the percentage of sulfate reduction in BR1 appeared to be correlated with temperature (Figure 11). This phenomenon was demonstrated in another study performed in 2018 by Nielsen et al. (2018). The highest overall percentage of sulfate removal occurred on August 29, 2020, at a rate of 97.0±0.2% and a temperature of 11.9±0.2°C. BR1 experienced the lowest annual removal rates on a seasonal basis in correspondence with late winter months (January – April) each year, where temperatures generally averaged between 5 and 10°C, with removal rates typically ranging from 20 to 50%. Contrastingly, summer and fall (June – October) generally displayed temperatures between 10 and 15°C, with typical removal rates between 50 to 90%. Summer 2020 consistently displayed the highest removal rates, with the majority of values >80%, while sulphate removal in the following summer had slightly lower values in general, typically in the range of 60-80%.

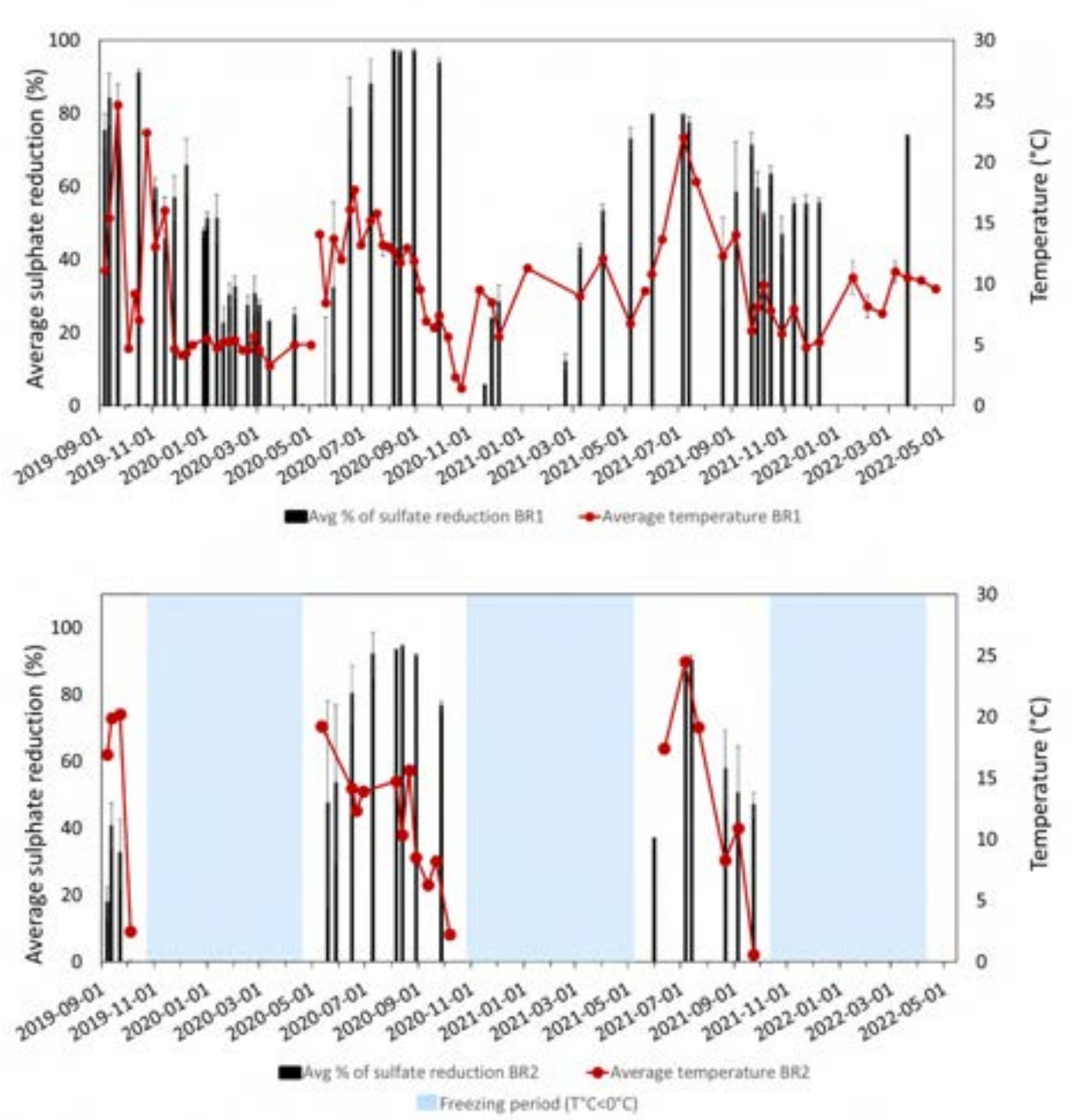

Figure 11:Positive percentage of sulfate removal of BR1 average and BR2 average, with the evolution of temperature within the BRs, function of time. The freezing period is represented in blue in BR2 chart.

Positive percentage of sulfate removal of BR1 average and BR2 average, with the evolution of temperature within the BRs, function of time. The freezing period is represented in blue in BR2 chart. Throughout the experiment, sulfate removal rates for BR2 average achieved seasonal lows on the first data point measured following the spring thaws, with 47.4±40.3% on May 19, 2020, and 36.9±0.0% on May 31, 2021. However, BR2 sulfate removal values consistently rebounded

within one or two measurements to mirror BR1 average values following thaw periods. Those results might indicate a slight delay between the increase in temperature and the increase in bacterial activity. The highest sulfate removal rate in BR2 was achieved on August 13, 2020, with a percentage of 94.1±0.4%, whereby August 2020 corresponded in general with the highest removal rates (>90%) of the study for both BR1 and BR2. The thaw period in 2021 was the last available data on sulfate removal in BR2 for the experiment.

4.6. Carbon

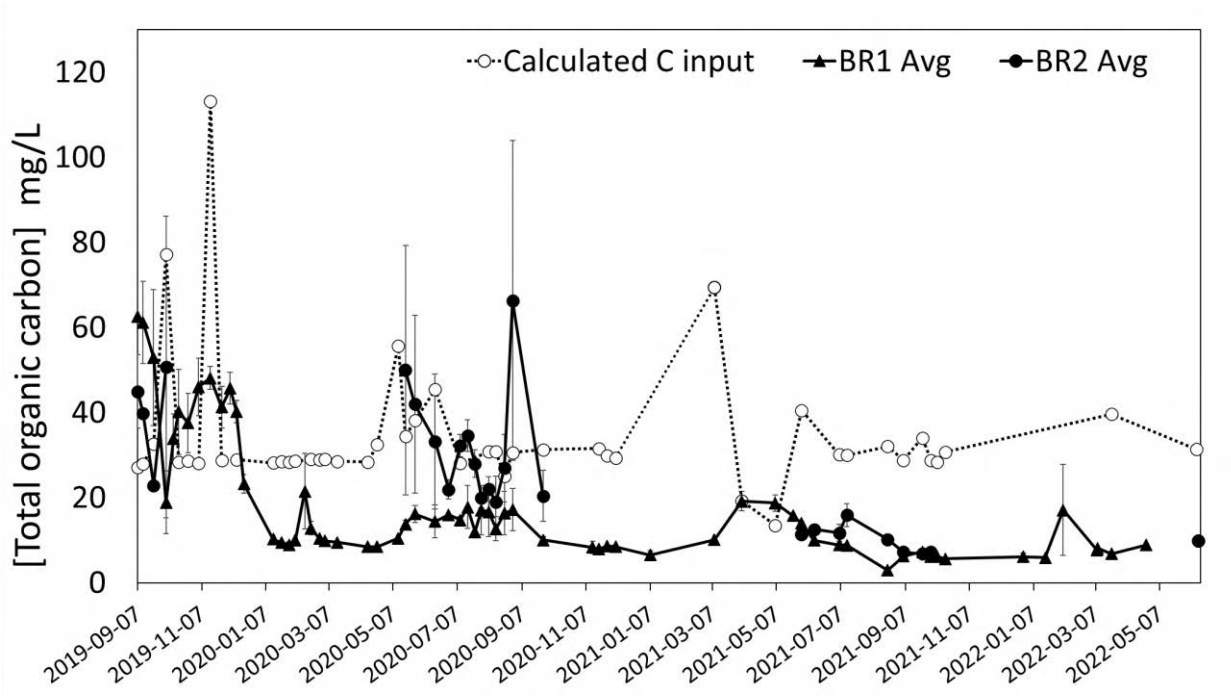

Figure 12: Carbon concentration, in mg/L, in the mine-contact water after molasses addition (Calculated C input, empty square and dashed line) and in the effluent of BR1 average BR1 Avg, black triangle and full line) and average BR2 (BR2 Avg, black circle and full line) function of time.

In order to support bacterial growth and efficiency, Total Organic Carbon (TOC) was injected in each BRs via a molasse solution. The estimated/calculated carbon addition was 25mg/L added to the initial TOC content in MCW.

Most of the total organic carbon detected in the MCW came from the molasses addition, otherwise the concentrations in carbon were usually quite low (<5 mg/L). Some spike events were detectable, mostly in the non-winter season. The fluctuations of MCW carbon concentrations could possibly be due to the changing of the MCW sample collection locations.

From the beginning of the experiment in September 2019 to December 2019, carbon concentration in BR1's effluent appeared to be higher than the TOC that was injected in the BRs, which translated into negative carbon percentage removal (figure 12). This was surprising as carbon consumption by targeted bacteria was expected. This phenomenon may be explained by potential carbon leaching by the spruce chips that were placed in each of the BRs to support biofilm growth. This hypothesis was assessed in a YukonU laboratory experiment where potential TOC leaching capacity of the wood chips used in the BRs was assessed in a column experiment. In this experiment, it was observed that spruce wood chips used to support biofilm growth leached 186.0 mg/L in column 1 and 154.0 mg/L in column 2 in the first week. For the total duration of the experiment of 8 weeks, the spruce wood chips leaching decreased to 26.6 mg /L in column 1 and 21.6 mg /L in column 2 (Annex 3).

In the meantime, carbon concentration in BR2 followed a similar trend compared to BR1 during fall 2019. However, when sampling BR2 was possible again after spring thaw 2020, it appeared that BR2 continued to leach carbon, as it can be observed in figure 13. This confirmed that the wood chips had a leaching capacity, throughout the first year of the study. However, the thaw period in 2021 showed exclusively positive values for BR2 carbon consumption, which continued for the duration of the experiment, and suggested that the wood chips' leaching capacity was longer adding carbon.

Although data was lacking for the BR2 average due to freezing periods, consumption values which had demonstrated high fluctuation during the first two years of the experiment stabilized throughout the final year of the study, when BR2 consumption rates began to closely mirror values in BR1, with an average of 68.3±3.3% in 2021 for BR2 and an average of 76.2±0.3% for BR1 during the same time period.

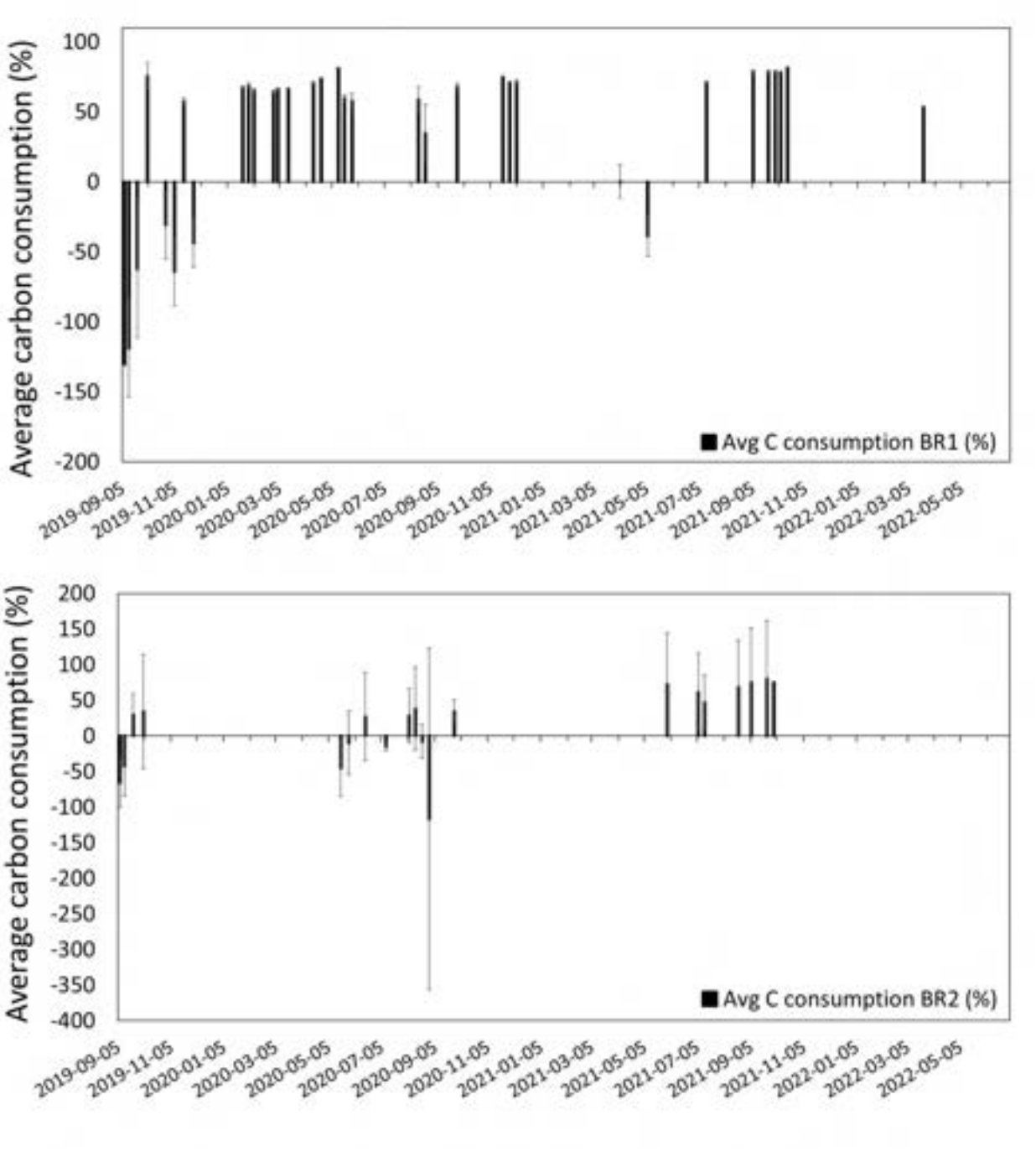

Figure 13: Percentage of carbon removal from BR1 average (top) and BR2 average (bottom) function of time.

4.7. Antimony

The concentration in antimony in the MCW and the effluent of BR1 average and BR2 average are presented in figure 14.

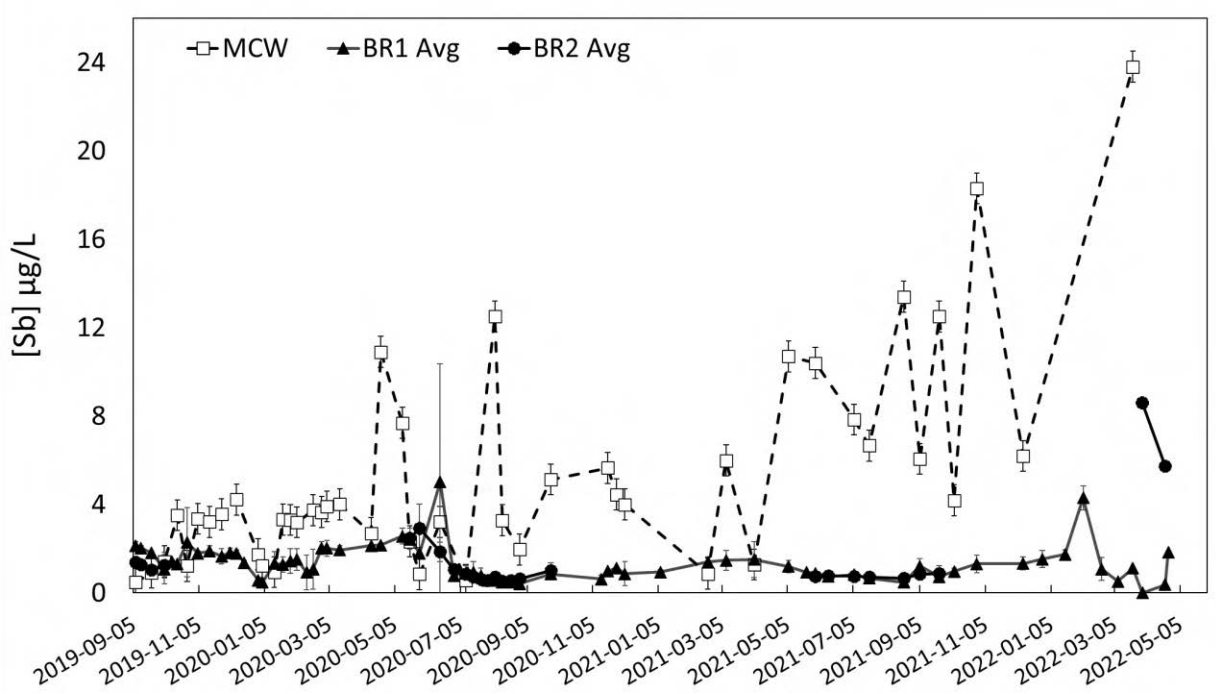

Figure 14: Antimony concentration in µg/L in mine-contact water (MCW, empty square and dashed line), average BR1 (BR1 Avg, black triangle and full line) and average BR2 (BR2 Avg, black circle and full line) function of time.

Antimony concentration of MCW was initially 0.48 µg/L on September 7, 2019, and steadily increased to 3.51 µg/L on October 16, 2019, where concentration remained relatively stable over the winter, with a low event in January that culminate at 0.94 µg/L on January 14, 2020. This lower event during winter was probably due to the change in the water source location. Antimony concentrations in MCW appeared to follow seasonal trends early in the study, which became less apparent in March 2021 when an increase in the variation between data points occurred and concentration levels, in general, began to follow an upward trend, reaching a high of 23.8 µg/L on March 22, 2022. Initially, Antimony concentration levels appeared to be more consistent during the winter months, with a higher proportion of extreme values during the summer.

During the first year of the study, the BR1 average Sb concentration generally mirrored the increases and fluctuations of MCW, as Sb values ranged from 0.48 to 7.69 µg/L, and BR1 average values spanned 0.48 to 5.05 µg/L from September 7, 2019 to September 27, 2020. BR1 average Sb concentration were consistently lower than the initial MCW Sb concentration, meaning that Sb was generally being removed during the BR process. This observation is highlighted in figure 15 which presents the percentage of Sb removal from BR1 average and BR2 average. As the concentration of Sb in MCW began to fluctuate with greater intensity during the project's second year, concentrations of Sb in BR1 average remained steady and consistent without any obvious response to the fluctuations. The highest Sb removal rate in BR1 was achieved on August 21, 2021, with an average of 96.4% of Sb removal while Sb concentration in MCW reached the maximal value of 23.8 µg/L on March 22, 2022. While Sb concentrations in MCW followed an upward trend throughout the study, it is interesting to note that this trend corresponded to steadily increasing removal in both BRs, ending with BR1 Sb removal rates consistently above 75% from May 2021 until the end of the study in early summer 2022, and BR2 removal rates above 85% for the same time period.

In the case of BR1 average, the average antimony removal for was positive except in ten cases. At the beginning of the experiment, the average concentration of Sb in BR1's effluent (2.15±0.13 µg/L) was higher than in the MCW (0.48 µg/L), which explained the negative value for Sb removal. The other negative Sb removal in BR1 was associated with low MCW values inferior to 1 µg/L, which might indicate a limitation of BR1 to remove Sb from MCW for low Sb concentration. It's however interesting to note that from the Quebec government website, the limit for contamination prevention of water and aquatic organisms is fixed at 6 µg/L, which would indicate that in case of Sb pollution event, BR1 would be able to remove enough Sb to limit the pollution event.

The BR2 average Sb concentrations were quite highly comparable to those detected for BR1 average when the BRs were not frozen. Before winter, on the 4th of October 2019, the concentration in Sb was 1.25±0.6 µg/L which is quite similar to the value detected at the beginning of the experiment (1.40±0.3 µg/L). Upon spring thaw, both BR1 and BR2 experienced negative removal values, which would indicate that it was not caused by the freezing of the outdoor BR2 tanks, since BR1 was not exposed to sub-zero temperatures.

Regarding Sb removal by BR2, the results were sparser since some data points are missing either for the MCW (such that removal rates could not be calculated) or the BR2 average due to sampling or analysis issues. The highest removal rate by BR2 was achieved on May 31, 2021, with 96.4±3.6%, which co-occurred with relatively high Sb concentrations detected in MCW. The similarity between the results obtained for BR1 average and BR2 average was also a good indication that despite the frozen state of BR2 average during winter, the BRs located outside were as effective for antimony removal as the BRs located inside. While antimony in MCW averaged to 5.20±4.7 µg/L over the course of the study, Sb concentrations in BR1 average were 1.33±0.8 µg/L and 1.53±0.2 µg/L for BR2, which suggested strong antimony removal capacity for both BRs.

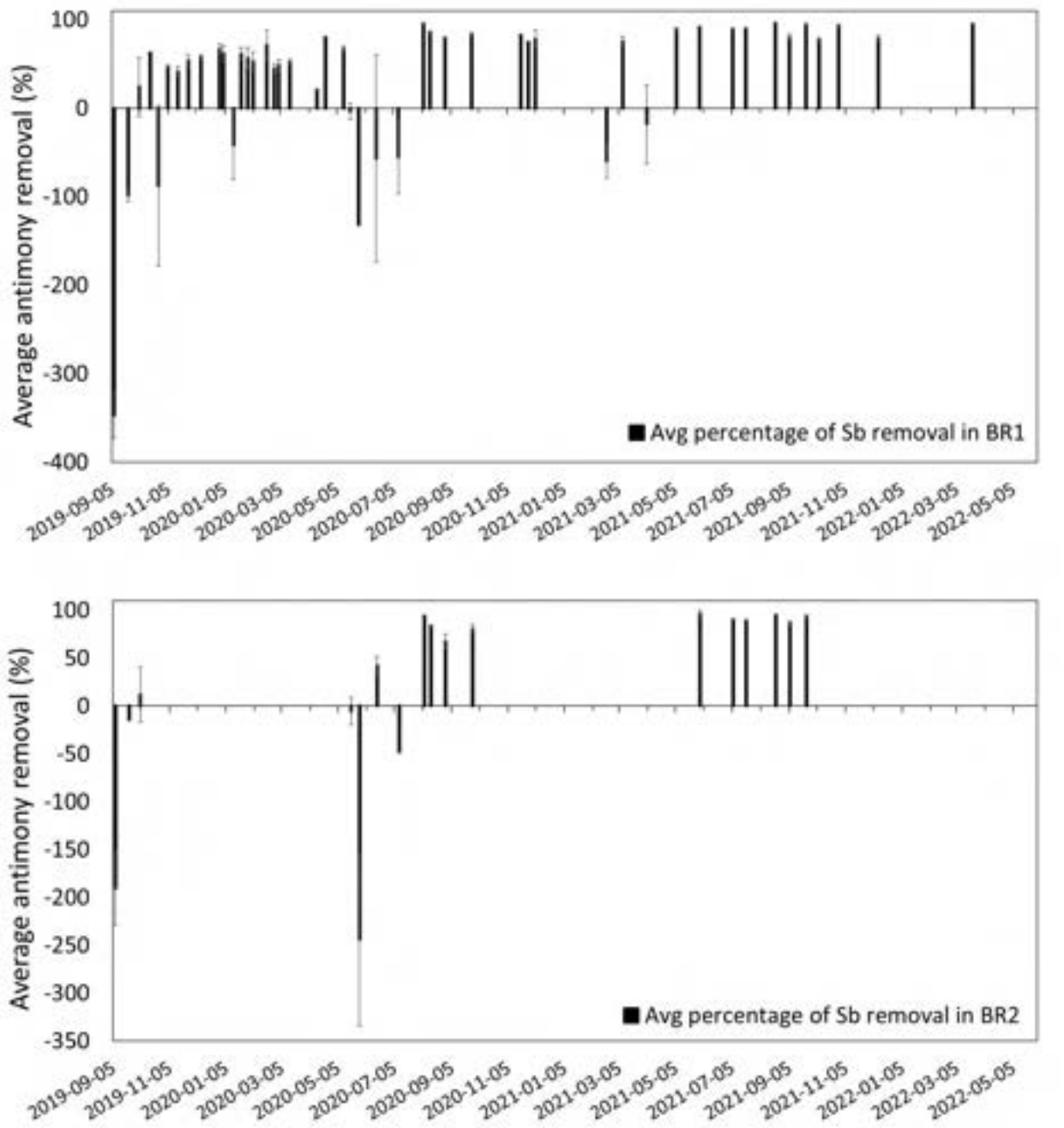

Figure 15: Percentage of antimony removal from BR1 average (top) and BR2 average (bottom) function of time.

4.8. Selenium

The concentration in Se in the MCW and the effluent of BR1 average and BR2 average are presented in figure 16.

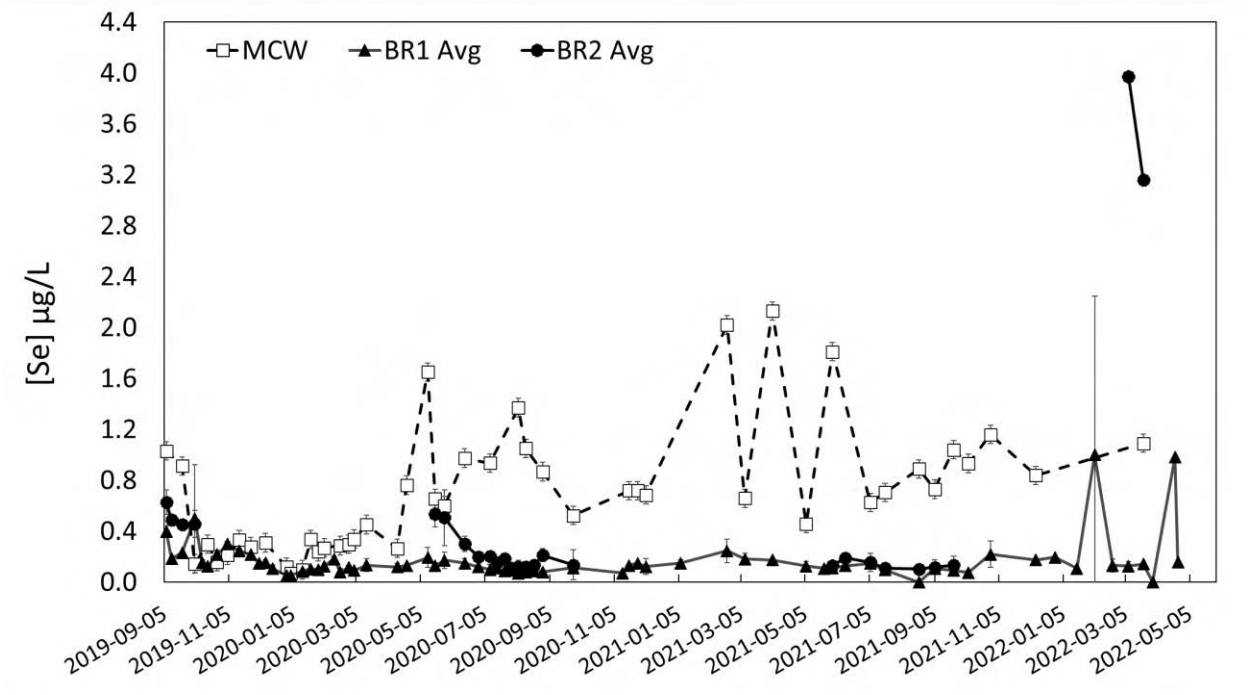

Figure 16: Antimony concentration in µg/L in mine-contact water (MCW, empty square and dashed line), average BR1 (BR1 Avg, black triangle and full line) and average BR2 (BR2 Avg, black circle and full line) function of time.

The initial Se concentration in MCW was 1.03 µg/L on September 7, 2019, with values ranging from as low as 0.07 µg/L on January 3, 2020, and as high as 2.13 µg/L on April 2, 2021. Concentrations of Se in MCW did not appear to follow any patterns related to seasonality, though followed a slight trend in positive growth and increasing variation throughout the experiment.

The initial Se concentration in BR1 average and BR2 average were 0.40±0.05 and 0.63±0.10 µg/L, respectively. Over the 3-year experiment, Se concentrations in BR1 average effluent were almost always under initial Se concentration in MCW, and remained relatively stable, comprised between 0.00 and 1.00 µg/L. The average percentage of Se removal for BR1 throughout the duration of the study was 60.6±7.6% (figure 17). There were three dates, two in October 2019 and one at the beginning of November 2019, where the percentage of removal were negative. As this specific behavior was not observed later, we can estimate that it is due to the initiation of the BRs. Thus, we can conclude than BR1 processes were efficient for Se removal. Although there was some initial variation in Se removal rates among the BR1 average, removal became increasingly consistent, with values above 70% from May 2020 to the end of the experiment. The highest removal percentage was obtained on the 21st of August 2021, with 100±0.0% of Se removed, and

the lowest (apart from negative value) was on the 14th of January 2020, with only 13.3±7.1% of Se removed.

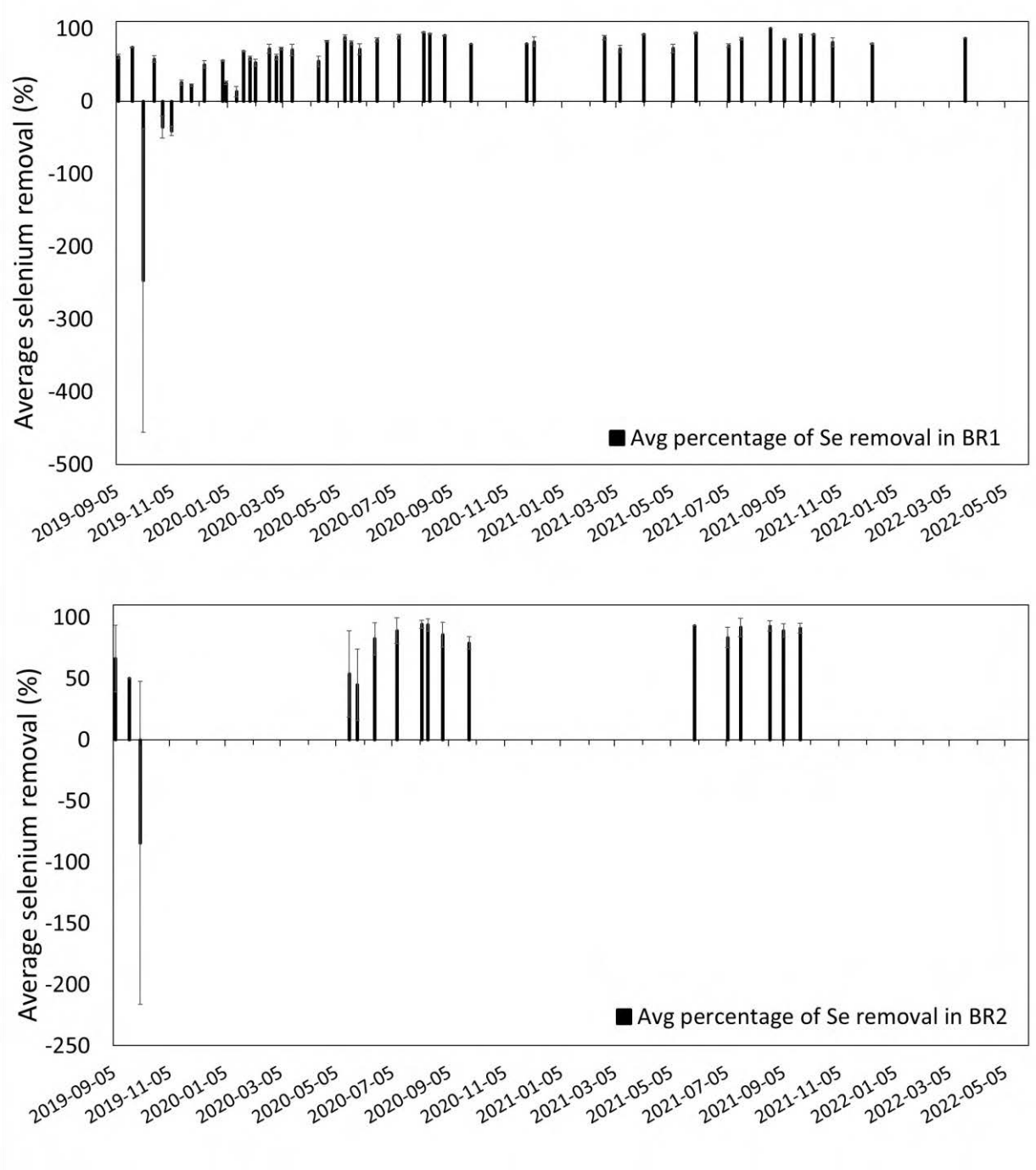

Figure 17: Percentage of antimony removal from BR1 average (top) and BR2 average (bottom) function of time.

Regarding BR2 average, it seemed that it behaved relatively similarly to BR1. Percentage removal rates in BR2 showed a marked increase in Se removal following freezing periods, where values increased from a negative removal value to 53.7±35% in spring 2020, and from 79.1±5.0% in fall 2020 to 93.0±0.0% in spring 2021. Se removal in BR2 became increasingly consistent throughout the experiment, remaining above 80% from June 2020 to the end of the study. This indicated that given some time to stabilize following the initiation of the BR, Se removal from MCW capacity was highly effective regardless of freezing periods. Indeed, the average removal of Se in BR2 during the duration of the study was 70.4±18%, which was higher than BR1's average removal rate (65.0±78%) during the thaw periods of the experiment.

Overall, the percentage of removal of Se for BR2 (figure 17) seemed to mirror the behavior of BR1 when it was unfrozen. The highest removal percentage was obtained on the same date as BR1 with the same value (94.3%) and the lowest one was obtained just after the thaw event on the 28th of May 2020, with a value of 44.8±29.3%. It is also interesting to note that the uncertainties estimated for BR2 average just after the thaw event were more important than during the rest of our study. This is due to higher discrepancy between the two duplicates of BR2 that might be explained by variation in the thawing speed or variation in microbial communities.

Given the similarity between the two percentages of removal obtained for BR1 average and BR2 average, we can assume that the freezing event undergone by BR2 did not affect its ability to remove Se from the MCW.

4.9. Arsenic

The evolution of arsenic concentrations in the MCW, BR1 average and BR2 average are presented in figure 18.

Surprisingly, arsenic concentrations were higher in BRs' effluent than in MCW, meaning that the BRs were releasing arsenic. The percentage of As removal was negative throughout the vast majority of measurements (data not shown) for both BR1 average and BR2 average.

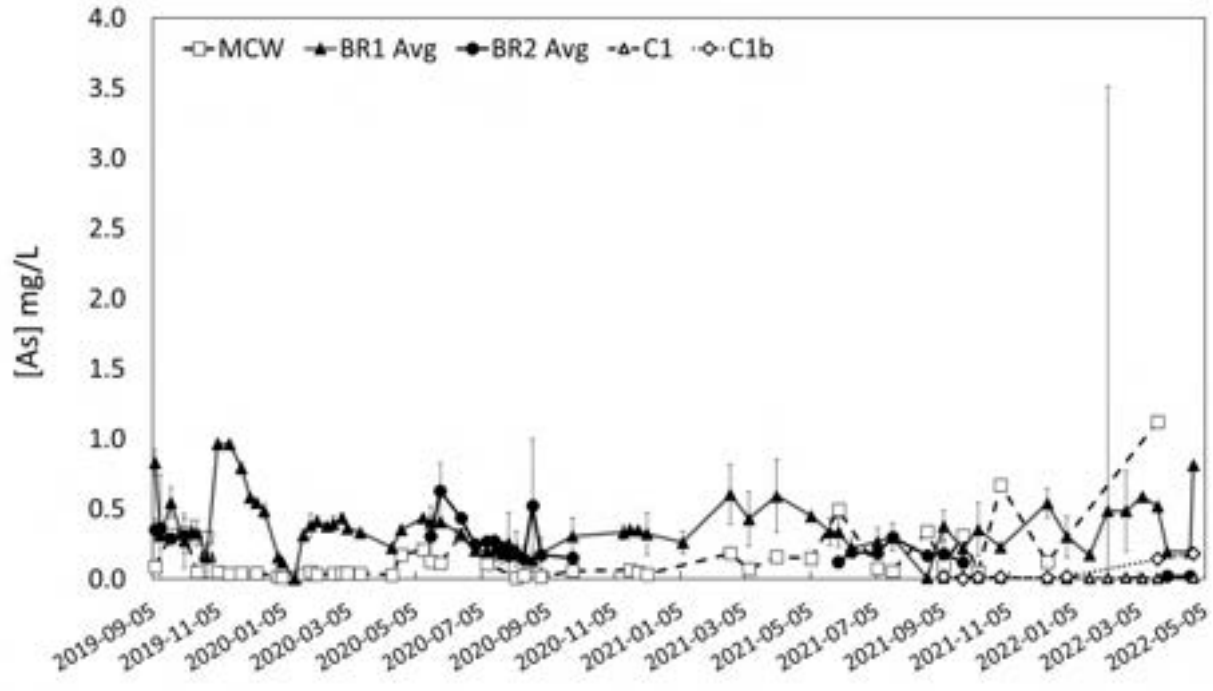

Figure 18 : Arsenic concentration in µg/L in mine-contact water (MCW, empty square and dashed line), average BR1 (BR1 Avg, black triangle and full line), average BR2 (BR2 Avg, black circle and full line), C1 (white triangle and dashed line), and C1b (white diamond and dashed line) function of time.

This came as a surprise, as it was expected that the BRs would be able to remove As. To explain those results, we performed leaching experiments to investigate (1) if the inoculum could be the source of As and (2) the speciation of As (to explain the release).

The As total metal, As(III) and As(V) concentration were measured in the distilled water used to perform the leaching, used as a blank, and for two sites (1 and 2) that corresponds to an average of two duplicates each, after 24 hours, 14 days and 30 days. The results per arsenic speciation are presented in figure 19.

The concentration in As (either total metal or As(III) or As(V)) in the distilled water (DIW) was always really low, indicating no or little contamination of the DIW with As. After 24 hours, the concentration in As at Site 1 and Site 2 were 0.062±0.016 mg/L and 0.082±0.014 mg/L. Regarding the speciation of As, the majority of As was present as As(V) for both Site 1 (0.044±0.011 mg/L) and Site 2 (0.063±0.012 mg/L) (figure 19-a). After 14 days of leaching, the total metal concentration in As dropped at 0.020±0.001 mg/L and 0.038±0.004 mg/L for Site 1 and Site 2, respectively. Associated to this important decrease in total metal As concentration, little or no As(III) were detected at both Site 1 and Site 2 (figure 19-b). Finally, after 31 days of experiment,

the concentration in As in solution increased up to 0.187±0.031 mg/L and 0.117±0.083 mg/L indicating an important release of As in the water (figure 19-c). Those results associated with the results at 14 days might indicate that sorption/desorption processes were taking place during the leaching experiment.

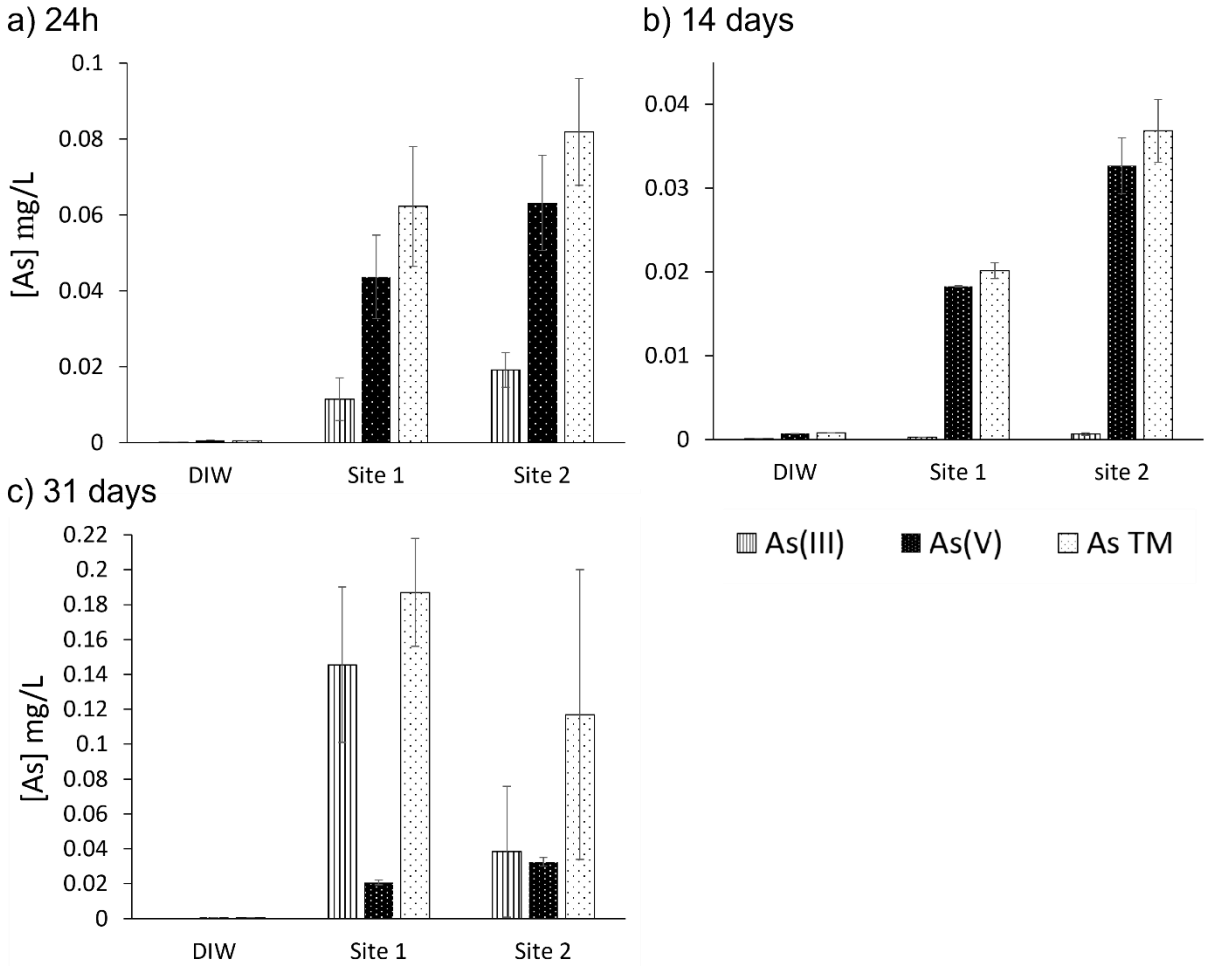

Figure 19: Average total metal (TM) As concentration, As(III) and As(V) in mg/L in the distilled water (DIW, vertical stripe), Site 1 (average value, black with white dot) and Site 2 (white with black dot) after 24 hours (a), 14 days (b) and 31 days (c). The y-axes are all in mg/L but the scales are different.

Regarding the speciation of As, the concentration in As(V) at 14 days and 31 days remained relatively constant with values around 0.02 mg/L and 0.03 mg/L for Site 1 and Site 2, respectively, which indicated a decrease of As(V) concentration after the first 24 hours which then stabilized over time. Conversely, the concentration in As(III) increased drastically after 31 days of exposure for both Site 1 and Site 2, with concentration of 0.145±0.044 mg/L and 0.038±0.037 mg/L,

respectively. The evolution in arsenic speciation over time was quite interesting since, as mentioned in the literature review, in oxic waters, As(V) is thermodynamically stable state, while As(III) is prevalent in reduced environments. Thus, As(III) is more mobile and toxic, in comparison to As(V). The fact that the total metal As concentration was much higher in the inoculum collected from Site 1 and Site 2 than in distilled water (DIW) over the course of the experiments indicated that the source of As in solution, and more largely the source of high As concentration in the BRs' effluent, was most likely the inoculum itself. The fact that As(V) was first released might indicate that the predominant form of As in the inoculum was As(V). The reducing condition observed in the BRs would favor the reduction of As(V) to As(III). Indeed, as previously mentioned, ORP measurements ranged from - 160.8mV (winter) to -378.2 mV (summer), which confirms the reducing conditions favorable to As(V) reduction. Those results are quite important and indicate that the BRs need to be complemented with another technique that will limit As release in the BRs' effluent. As Fe concentrations (annex 1) in MCW were relatively low through the three-year experiment, the addition of iron coated sand in the bioreactor matrix could be investigated to overcome this issue. The hypothesis is that As(III) could be adsorbed by the FeS and then incorporated into the FeS crystal structure to form Arsenopyrite (FeAsS).

Columns C1 and C1b were installed in series of BR1 and BR1b in order to treat specifically the As leaching phenomenon discussed above. Both columns were filled with Zero Valent Iron (ZVI) particles (i.e., Fe°). Fe° is a metallic form of iron which is frequently used in environmental remediation and as a component of permeable reactive barriers (PRBs) to remove various contaminant, including As. Different processes can occur that favor As removal. As can be directly adsorbed at the surface of the ZVI. Another mechanism relies on the transformation of the ZVI to iron oxides phases. The product of ZVI corrosion either incorporate As into their structure (coprecipitation) or adsorb As onto their surface. In anaerobic conditions, which are the conditions of this study, As removal is attributed to adsorption on the surface of corroded ZVI (Lackovic *et al.* 2000; Melitas *et al.* 2002; Lien and Wilkin 2004). A previous study conducted by the Northern Mine Remediation team focusing on the utilization of permeable reactive barrier made of ZVI showed As removal rate superior to 95% over the 9-months experiments [1].

[1] https://www.yukonu.ca/sites/default/files/inline-files/RENR401_FinalReport_0.pdf

The C1 column was filled to 100% of its total volume with ZVI, while the C1b column was filled to 50%. Data collection in the ZVI columns spanned from September 2021 to the end of the study, with fewer data points for the C1b column due to clogging issues with the column (January – March 2022). As concentrations in C1 ranged from 0.0033 mg/L on December 28, 2021, to 0.021 mg/L on September 23, 2021. Values for C1b ranged from 0.0022 mg/L on September 23, 2021, to 0.18 mg/L on April 24, 2022. The average As concentration in C1 throughout the experiment was 0.0078±0.0048 mg/L, with an average of 0.050±0.065 mg/L for C1b. As concentrations within the ZVI columns were consistently lower and less variable than those with BR1 and BR1b. The percentage of As removal for the ZVI columns was calculated using the concentration of the effluent of BR1 and BR1b as the influent. The percentage of As removal was comprised between 97.2% and 99.2% for C1, with one outlier at 52.9% in August 2022. For C1b, who stopped working in April 2022, the As removal is comprised between 69.3% and 98.5%, with the two lower values of 69.3% and 79.3% occurring just before the dismantlement of the column, indicating that the decrease of As removal is possibly link to the clogging of the column. The percentage removal of C1B during its activities is 90±10% against 94±13% for C1, indicating a small impact of the packing method on the percentage of removal. Overall, these results indicated good As removal capabilities of the ZVI columns.

4.10. Other potentially toxic elements

Figure 20 presents the concentration for four different elements that are usually considered as potentially toxic in the environment: Zn (figure 20-a), Cu (figure 20-b), Cd (figure 20-c) and Pb (figure 20-d). Even though those elements were not presented at concentration level high enough in the MCW to represent a source of contaminants in the environment, it's interesting to note that their concentrations in the MCW varied over the 3-year experiment. The concentration in those four elements was most of the time quite low, except for some "higher" event, easily noticeable on our charts, and often particular to MCW without reflection in BR effluent. While the higher events for Cd and Pb seemed to be related in time, for Zn and Cu no specific trend was observed. The concentration in the four elements in BR1 average and BR2 average were generally inferior to the concentration detected in the MCW in the case of those potentially toxic elements.

It is quite interesting to note that in both cases, BR1 average and BR2 average (when thawed), the BRs were able to efficiently remove the four potentially toxic elements. It appeared similar to what was observed for Se, where the concentration in BR2 average directly the following thaw was slightly higher than for BR1, which may indicate that the "re-start" of the BRs located outside was a bit slower than the BRs who did not freeze during winter. However, for Se, the removal efficiency was consistently promising.

Those results were a good indicator of the viability of such BRs, inoculated with local microbial population and possibly inactive over winter, to limit the release of most potentially toxic elements contained in MCW in to the environment.

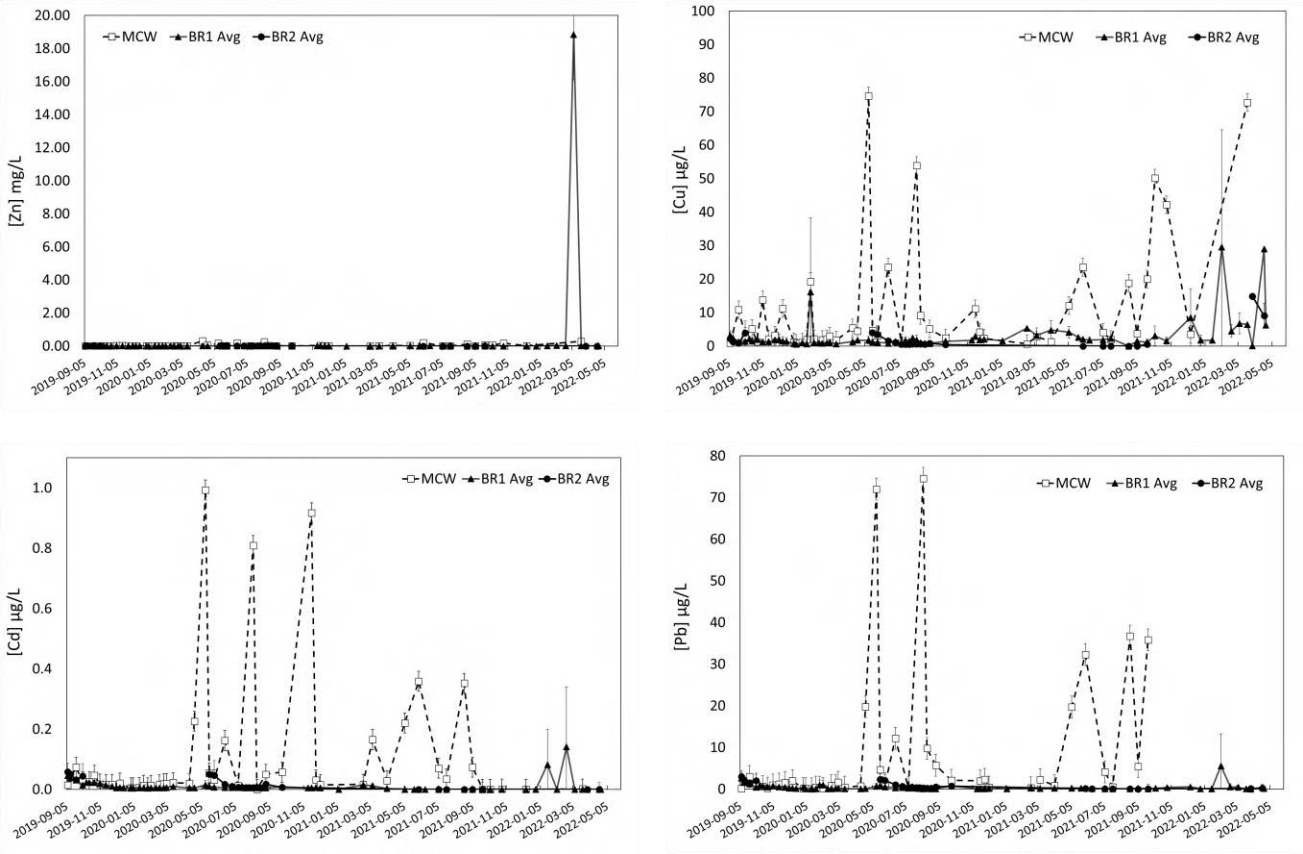

Figure 20: Concentration in Zn in mg/L (a), in Cu in µg/L (b), in Cd in µg/L (c) and in Pb in µg/L (d) in the mine-contact water (MCW, empty square and dashed line), average BR1 (BR1 Avg, black triangle and full line) and average BR2 (BR2 Avg, black circle and full line) function of time.

5. Conclusion

The goal of this study was to investigate at the pilot scale the utilization of bioreactors inoculated with Yukon native bacteria sampled from Eagle Gold mine site to limit water pollution and to study the adaptably of those bacteria to seasonal freeze and thaw cycles. To do so, two sets of two bioreactors each were built indoor and outdoor of a shed on the Eagle Gold mine site, and mine-contact water was flushed through it over three years. The concentration of various chemical elements and water characteristics were measured several times per month in the source, the mine-contact water, and the effluent of the different bioreactors. The results obtained for the set of bioreactors outside and the set of bioreactors inside were averaged. The bioreactors set up outside were frozen over winter, so no data were recorded during freezing periods from mid-October to mid-May.

Bacteria's activity was first assessed by studying sulfate reduction and carbon consumption. Sulfate reduction was correlated with temperature which might be a strong indicator of bacterial activity being lower during wintertime and higher during summertime, as already described in Nielsen et al., 2018. The bioreactors located outside presented a similar behavior to the one located inside.

The carbon consumption was more complicated to discuss, since some leaching occurred from the wood chips added in the bioreactors.

The Ca concentration present a seasonal cyclicity, with high concentration during winter and lower concentration during summer. This seasonal evolution may be due to concentration/dilution processes link to the variation in water level.

Bacterial capacity to remove As, Se and Sb (POC highlighted by Victoria Gold) from the MCW were investigated. Se and Sb removal by the BRs system is promising, with relatively high removal rate for both elements. The highest removal rate was reached over summer 2020, with removal values superior to 90% for both elements. For Se, it looked similar to sulfate reduction, the removal was higher over summer and lower in winter. Once again, the bioreactors located outside seems to behave similarly to those located inside, except for the period following the spring thaw where for

a couple of weeks, the removal rate are a bit lower for the bioreactors outside compared to the bioreactors inside.

Regarding As, the removal rate was most of the time negative, which indicated a release of As in the BRs' effluent. This unexpected phenomenon may be explained by As(V), the main form of As in the inoculum, being reduced to As(III) inside the bioreactors. The addition of iron coated sand at the exit of the bioreactors have been investigated in the last year of the experiment, showing promising results with an important decrease in As concentration. During the ZVI columns activity, the concentration in As are lower in the columns' effluent than in the influent. Methods for addressing As leaching from inoculum should be considered and incorporated into future bioreactor applications.

Finally, the study of other potentially toxic elements like Cu, Pb, Zn and Cd showed that the bioreactors used in this study can efficiently remove those elements from the contaminated water.

Globally the bioreactors demonstrated their ability to remove most contaminants from mine-contact water. The removal was due to the bacterial activity detectable through sulfate reduction. The rate of removal seemed to be related to the temperature and thus, bacterial activity, with higher removal during summer and lower removal during winter. More importantly, the seasonal freezing of the bioreactors located outside did not seem to affect their ability to remove the targeted elements.

6. References

Andreae MO. 1980. Arsenic in rain and the atmospheric mass balance of arsenic. GeoPhys Res. 85(C8): 4512-4518.

Besser JM, Canfield TJ, La Point TW. 1993. Bioaccumulation of organic and inorganic selenium in a laboratory food chain. Env Toxic. 12: 57-72.

Bissen M, Frimmel FH, 2003. Arenic-a review. Part 1: occurrence, toxicity, speciation, mobility. Acta Hydrochim Hydrobiol. 31(1): 9-18.

Boyle RW, Jonasson IR. 1973. The geochemistry of arsenic and its use as an indicator element in geochemical prospecting. Geochem Expl. 2(3): 251-296.

Castro JM, Wielinga BW, Gannon JE, Moore JN. 1999. Stimulation of sulfate-reducing bacteria in lake water from a former open-pit mine through addition of organic wastes. Wat Env Res. 71(2): 218-223.

Coughtrey PJ, Jackson D, Thorne MC. 1983. Radionuclide distribution and transport in terrestrial and aquatic ecosystems, Vol. 3. AA Balkema, Rotterdam.

Filella M, Belzile N, Chen YW. 2002. Antimony in the environment: A review focused on natural waters: II. Relevant solution chemistry. Earth-Sci Rev. 59(1-4): 265-285.

Fujita M, Ike M, Kashiwa M, Hashimoto R, Soda S. Laboratory-scale continuous reactor for soluble selenium removal using selenate-reducing bacterium, Bacillus sp. SF-1. Biotech Bioeng. 80(7): 755-761.

Gibert, O., Pablo, Jd, Cortina, J.L., Ayora, C., 2002. Treatment of acid mine drainage by sulphate-reducing bacteria using permeable reactive barriers: a review from laboratory to full scale experiments. Rev. Environ. Sci. Biotechnol. 1, 327e333.

Gloyna EF (1972) Waste stabilization ponds. World Health Organization, Geneva, Swiss, 175 p.

Harerimana, C., Harbi, B., Vasel, J., 2010. Development of a stoichiometric model of the sulphate-reduction by the sulphate-reducing bacteria in anaerobic lagoons. Biotechnol. Agron. Soc. Environ. 14, 577e582.

Health Canada. 1992. Guidelines for Canadian Drinking Water Quality. Supporting Document – Selenium. April, 1979. Updated December 1992.

Hozhina EI, Kramov AA, Gerasimov PA, Kumarkov AA. 2001. Uptake of heavy metals, arsenic, and antimony by aquatic plants in the vicinity of ore mining and processing industries. Geochem Expl. 74: 153-162.

Hunter WJ, Kuykendall LD, Manter DK. 2007. Rhizobium selenireducens sp. nov.: A selnite-reducing a-Proteobacteria Isolated from a Bioreactor. Curr Microbiol. 55: 455-460.

Janin A., Ness I. and Wilbur S. 2015. Arsenic, Antimony and Selenium Removal from Mine Water by Anaerobic Bioreactors at Laboratory Scale, May 2015.

Jong T, Parry DL. 2003. Removal of sulfate and heavy metals by sulfate reducing bacteria in short-term bench scale upflow anaerobic packed bed reactor runs. Wat Res. 37: 3379-3389.

Khairul I, Wang QQ, Jiang YH, Wang C, Naranmandura H. 2017. Metabolism, toxicity and anticancer activities of arsenic compounds. Oncotarget. 8(14): 23905-23926.

Khamkhash A, Srivastava V, Ghosh T, Akdogan G, Ganguli R, Aggarwal S. 2017. Mining-related selenium contamination in Alaska, and the state of current knowledge. Min. 7(3):1-13.

Komesli OT. 2014. Removal of heavy metals in wastewater by membrane bioreactor: Effects of flux and suction period. Chem Soc Paki. 36(4): 654-659.

Korte NE, Fernando Q. 2009. A review of arsenic (III) in groundwater. Crit Rev Env Cont. 21(1): 1-39.

Lackovic JA, Nikolaidis NP, Dobbs GM. 2000. Inorganic arsenic removal by zero-valent iron. Environ Eng Sci 17(1):29-39.

Lemly AD. 2004. Aquatic selenium pollution is a global environmental safety issue. Ecotox & Env Safe. 59: 44-56.

Lien H and Wilkin RT. 2005. High-level arsenite removal from groundwater by zero-valent iron. Chemosphere 59(3):377-86.

Liu F, Le XC, McKnight-Whitford A, Xia Y, Wu F, Elswick E, Johnson CC, Zhu C. 2010. Antimony speciation and contamination of waters in the Xikuangshan antimony mining and smelting area, China. Env Geochem Health. 32: 401-413.

Liu F, Zhang G, Liu S, Fu Z, Chen J, Ma C. 2018. Bioremoval of arsenic and antimony from wastewater by a mixed culture of sulfate-reducing bacteria using lactate and ethanol as carbon sources. Int Biodeter Biodeg. 126: 152-159.

Matschullat J. 2000. Arsenic in the geosphere – a review. Sci Tot Env. 249(1-3): 297-312.

Melitas N, Wang J, Conklin M, O'Day P, Farrell J. 2002. Understanding soluble arsenate removal kinetics by zerovalent iron media. Environ Sci Technol 36(9):2074-81.

Mine Environment Neutral Drainage (MEND) Program. 2004. Review of water quality issues in neutral pH drainage: examples and emerging priorities for the mining industry in Canada. MEND Report 10.1. Prepared by Stantec Consulting Ltd. (Brampton). November 2004.

Mine Environment Neutral Drainage (MEND) Program. 2007. A review of environmental management criteria for selenium and molybdenum. MEND Report 10.1.1. Prepared by Ecometrix Inc. (Brampton). November 2007.

Mitsunobu S, Takahashi Y, Terada Y, Sakata M. 2010. Antimony (V) incorporation into synthetic ferrihydrite, goethite, and natural iron oxyhydroxides. Env Sci Tech. 44(10): 3712-3718.

Nielsen, G., Hatam, I., Abuan, K. A., Janin, A., Coudert, L., Blais, J. F., ... & Baldwin, S. A. (2018). Semi-passive in-situ pilot scale bioreactor successfully removed sulfate and metals from mine-contact water under subarctic climatic conditions. Water research, 140, 268-279.Obiakor MO, Tighe M, Pereg L, Wilson SC. 2018. Bioaccumulation, trophodynamics and ecotoxicity of antimony in environmental freshwater food webs. Crit Rev Env Sci & Tech. 0(0): 1-51.

Ogle RS, Maler KJ, Kiffney P, Williams MJ, Brasher A, Melton LA, Knight AW. 1988. Bioaccumulation of selenium in aquatic ecosystems. Lake & Res Mgmt. 4(2): 165-173.

Okkenhaug G, Zhu YG, Luo L, Lei M, Li X, Mulder J. 2011. Distribution, speciation and availability of antimony (Sb) in soils and terrestrial plants from an active Sb mining area. Env Poll. 159(10): 2427-2434.

Oorts K, Smolders E, Degryse F, Buekers J, Gasco G, Cornelius G, Mertens J. 2008. Solubility and toxicity of antimony trioxide (Sb2O3) in soil. Env Sci Tech. 42(12): 4378-4383.

Rahman MA, Hasegawa H, Lim RP. 2012. Bioaccumulation, biotransformation and trophic transfer of arsenic in the aquatic food chain. Env Res. 116: 118-135.

Ritchie VJ, Ilgen AG, Mueller SH, Trainor TP, Goldfarb RJ. 2013. Mobility and chemical fate of antimony and arsenic in historic mining environments of the Kantishna Hills district, Denali National Park and Preserve, Alaska. Chem Geol. 335(6): 172-188.

Roussel C, Neel C, Bril H. 2000. Minerals controlling arsenic and lead solubility in an abandoned gold mine tailings. Sci Total Env. 263: 209-219.

Sanchez-Castro I, Bakkali M, Merroun ML. 2017. Draft genome sequence of Stenotrophomonas bentonitica BII-R7T, a selenite-reducing bacterium isolated from Spanish bentonites. Microbiol Res Annou. 5(31): e00719-17

Simonton S, Dimsha M, Thomson B, Barton LL, Cathey G. Long-term stability of metals immobilized by microbial reduction. Proceedings of the 2000 Conference on Hazardous Waste Research: Environmental Challenges and Solutions to Resource Development, Production and Use, Southeast Denver, CO, 2000. p. 394-403.

Stauder S, Raue B, Sacher F. 2005. Thioarsenates in sulfidic waters. Env Sci Tech. 39(16): 5933-5939.

Sun W, Xiao E, Kalin M, Krumins V, Dong Y, Ning Z, Liu T, Sun M, Zhao Y, Wu S, Mao J, Xiao T. 2016. Remediation of antimony-rich mine waters: Assessment of antimony removal and shifts in the microbial community of an onsite field-scale bioreactor. Env Poll. 215: 213-222.

Thomas DJ, Styblo M, Lin S. 2001. The cellular metabolism and systemic toxicity of arsenic. Toxic App Pharma. 176(2): 127-144.

Tolonen ET, Rämö J, Lassi U (2015) The effect of magnesium on partial sulphate removal from mine water as gypsum. J Environ Manag 159:143-146.

Trumm D, Ball J, Pope J, Weisener C. Antimony passive treatment by two methods: Sulfate reduction and adsorption onto AMD precipitate. In: Adrian Brown. 10th International Conference on Acid Rock Drainage & IMWA Annual Conference; April 21-24, 2015; Santiage, Chile. Santiago, Chile: Gecamin Ltda; 2015. p.1-9.

Uhrie JL, Drever JI, Colberg PJS, Besbitt CC. 1996. In situ immobilization of heavy metals associated with uranium leach mines by bacterial sulfate reduction. Hydrometallurgy. 43: 231-239.

Wang H, Chen F, Mu S, Zhang D, Pan X, Lee DJ, Chang JS. 2013. Removal of antimony (Sb(V)) from Sb mine drainage: Biological sulfate reduction and sulfide oxidation-precipitation. BioRes Tech. 146: 799-802.

Webster J. 1990. The solubility of As2S3 and speciation of As in dilute and sulfide-bearing fluids at 25 and 90C. Geochem Cosmochem Acta. 54: 1009-1017.

Zhang G, Ouyang X, Li H, Fu Z, Chen J. 2016. Bioremoval of antimony from contaminated waters by a mixed batch culture of sulfate-reducing bacteria. Int Biodet & Biodeg. 115: 148-155.

7. Appendixes

Annex 1: ALS Certificate of Analysis

ALS Environmental

CERTIFICATE OF ANALYSIS

Work Order	WR2000592	Page	1 of 4
Client	Victoria Gold (Yukon) Corp.	Laboratory	Whitehorse - Environmental
Contact	Katie Bolon	Account Manager	Hilary Woods
Address	Suite 1000 - 1050 W. Pender St. Vancouver BC Canada V6E 3S7	Address	#12 151 Industrial Road Whitehorse YT Canada Y1A 2V3
Telephone	867.456.7720 ext. 8308	Telephone	+1 867 668 8868
Project	BIOREACTOR JUL 30	Date Samples Received	03-Aug-2020 09:35
PO	14049	Date Analysis Commenced	05-Aug-2020
C-O-C number	20200801a	Issue Date	11-Aug-2020 11:48
Sampler	KTLU		
Site	---		
Quote number	Q55100		
No. of samples received	4		
No. of samples analysed	4		

This report supersedes any previous report(s) with this reference. Results apply to the sample(s) as submitted. This document shall not be reproduced, except in full.

This Certificate of Analysis contains the following information:

- General Comments
- Analytical Results

Additional information pertinent to this report will be found in the following separate attachments: Quality Control Report, QC Interpretive report to assist with Quality Review and Sample Receipt Notification (SRN).

Signatories

This document has been electronically signed by the authorized signatories below. Electronic signing is conducted in accordance with US FDA 21 CFR Part 11.

Signatories	Position	Laboratory Department
Kim Jensen	Department Manager - Metals	Metals, Burnaby, British Columbia
Tracy Horley	Supervisor - Water Quality Instrumentation	Inorganics - Water Quality, Burnaby, British Columbia

RIGHT SOLUTIONS | RIGHT PARTNER

General Comments

The analytical methods used by ALS are developed using internationally recognized reference methods (where available), such as those published by US EPA, APHA Standard Methods, ASTM, ISO, Environment Canada, BC MOE, and Ontario MOE. Refer to the ALS Quality Control Interpretive report (QCI) for applicable references and methodology summaries. Reference methods may incorporate modifications to improve performance.

Where a reported less than (<) result is higher than the LOR, this may be due to primary sample extract/digestate dilution and/or insufficient sample for analysis.

Where the LOR of a reported result differs from standard LOR, this may be due to high moisture content, insufficient sample (reduced weight employed) or matrix interference.

Please refer to Quality Control Interpretive report (QCI) for information regarding Holding Time compliance.

Key: CAS Number: Chemical Abstracts Services number is a unique identifier assigned to discrete substances.
LOR: Limit of Reporting (detection limit).

Unit	Description
ng/L	nanograms per litre

< : less than.

> : greater than.

Surrogate: An analyte that is similar in behavior to target analyte(s), but that does not occur naturally in environmental samples. For applicable tests, surrogates are added to samples prior to analysis as a check on recovery.

Test results reported relate only to the samples as received by the laboratory.

UNLESS OTHERWISE STATED on QRN or QCI Report, ALL SAMPLES WERE RECEIVED IN ACCEPTABLE CONDITION.

Analytical results in reports identified as "Preliminary Report" are considered authorized for use.

Qualifiers

Qualifier	Description
DLR	Detection Limit Adjusted due to sample matrix effects (e.g. chemical interference, colour, turbidity)

Analytical Results

Sub-Matrix: Water
(Matrix: Water)

Analyte	CAS Number	Method	LOR	Unit	Client sample ID: BR1	BR1b	BR2	BR2b	---
					Client sampling date / time: 30-Jul-2020 09:30	30-Jul-2020 09:40	30-Jul-2020 09:55	30-Jul-2020 10:00	---
					WR2000592-001	WR2000592-002	WR2000592-003	WR2000592-004	------
					Result	Result	Result	Result	---
Physical Tests									
hardness (as CaCO3), from total CaMg	----	EC100A	0.83	mg/L	149	127	112	117	---
Anions and Nutrients									
sulfate (as SO4)	14808-79-8	E235.SO4	0.30	mg/L	1.30	2.65	7.67	7.46	---
Organic / Inorganic Carbon									
carbon, total organic [TOC]	----	E355-L	0.50	mg/L	22.6	11.3	17.8	22.3	---
Total Metals									
aluminum, total	7429-90-5	E420	0.0030	mg/L	0.0309	0.0249	0.0852	0.119	---
antimony, total	7440-36-0	E420	0.00010	mg/L	0.00057	0.00054	0.00059	0.00059	---
arsenic, total	7440-38-2	E420	0.00010	mg/L	0.409	0.108	0.167	0.161	---
barium, total	7440-39-3	E420	0.00010	mg/L	0.139	0.0956	0.139	0.140	---
beryllium, total	7440-41-7	E420	0.000010	mg/L	0.000031	0.000021	<0.000010	0.000022	---
bismuth, total	7440-69-9	E420	0.000050	mg/L	<0.000050	<0.000050	<0.000050	0.000051	---
boron, total	7440-42-8	E420	0.010	mg/L	<0.010	<0.010	<0.010	<0.010	---
cadmium, total	7440-43-9	E420	0.0000050	mg/L	<0.0000050	<0.0000050	0.0000066	0.0000060	---
calcium, total	7440-70-2	E420	0.050	mg/L	42.1	36.4	34.8	35.6	---
chromium, total	7440-47-3	E420 Cr-L	0.00010	mg/L	0.00032	0.00032	0.00033	0.00033	---
cobalt, total	7440-48-4	E420	0.00010	mg/L	0.00023	0.00018	0.00112	0.00094	---
copper, total	7440-50-8	E420	0.00050	mg/L	0.00215	0.00208	<0.00050	0.00215	---
iron, total	7439-89-6	E420	0.010	mg/L	9.68	4.55	8.83	10.4	---
lead, total	7439-92-1	E420	0.000050	mg/L	0.000101	0.000166	0.000271	0.000429	---
lithium, total	7439-93-2	E420	0.0010	mg/L	0.0049	0.0041	0.0029	0.0034	---
magnesium, total	7439-95-4	E420	0.100	mg/L	10.0	8.79	9.16	9.68	---
manganese, total	7439-96-5	E420	0.00010	mg/L	0.927	0.394	0.987	1.46	---
molybdenum, total	7439-98-7	E420	0.000050	mg/L	0.000191	0.000210	0.000168	0.000340	---
nickel, total	7440-02-0	E420	0.00050	mg/L	0.00051	<0.00050	<0.00050	0.00058	---
phosphorus, total	7723-14-0	E420	0.050	mg/L	<0.050	0.056	<0.050	<0.050	---
potassium, total	7440-09-7	E420	0.100	mg/L	4.42	3.59	2.43	3.19	---
selenium, total	7782-49-2	E420	0.000050	mg/L	0.000110	0.000077	0.000068	0.000130	---
silicon, total	7440-21-3	E420	0.10	mg/L	5.29	5.12	5.23	5.82	---
silver, total	7440-22-4	E420	0.000010	mg/L	<0.000010	<0.000010	0.000010	<0.000010	---
sodium, total	7440-23-5	E420	0.050	mg/L	2.40	2.52	2.28	2.28	---

Analytical Results

Sub-Matrix: Water
(Matrix: Water)

Analyte	CAS Number	Method	LOR	Unit	Client sample ID: BR1	BR1b	BR2	BR2b	---
					Client sampling date / time: 30-Jul-2020 09:30	30-Jul-2020 09:40	30-Jul-2020 09:55	30-Jul-2020 10:00	---
					WR2000592-001	WR2000592-002	WR2000592-003	WR2000592-004	------
					Result	Result	Result	Result	---
Total Metals									
strontium, total	7440-24-6	E420	0.00020	mg/L	0.240	0.204	0.208	0.224	---
sulfur, total	7704-34-9	E420	0.50	mg/L	<0.50	1.19	2.45	2.52	---
thallium, total	7440-28-0	E420	0.000010	mg/L	<0.000010	<0.000010	<0.000010	<0.000010	---
tin, total	7440-31-5	E420	0.00010	mg/L	<0.00010	<0.00010	<0.00010	<0.00010	---
titanium, total	7440-32-6	E420	0.00030	mg/L	0.00169	0.00209	0.00244	<0.00030 **	---
uranium, total	7440-61-1	E420	0.000010	mg/L	0.000217	0.000299	0.000120	0.000251	---
vanadium, total	7440-62-2	E420	0.00050	mg/L	0.00113	0.00101	0.00089	0.00074	---
zinc, total	7440-66-6	E420	0.0030	mg/L	0.0101	0.0062	0.0038	0.0119	---
zirconium, total	7440-67-7	E420	0.00030	mg/L	0.00062	0.00061	0.00036	0.00057	---

Please refer to the General Comments section for an explanation of any qualifiers detected.

Annex 2: Sampling protocol & Bioreactor maintenance

Refer to **Pilot scale Bioreactors at Eagle Gold Mine site**

In case of any problems or emergency, contact **Guillaume Nielsen 581-307-1985**

	DATE (yyyy/mm/dd)	2/19/2020		NAME	JW, PE	
1	Shed room temperature				5°C	
2	Outside Temperature				-8'°C	
3	Source of MCW				LDSP Well	
4	Hours Tracking Log Filled out?				Yes	
		Fresh MCW	BR1	BR1b	BR2	BR2b
5	Volume of treated water in outlets (L)		20L	80L	L	L
6	Stirring the treated water in outlets with PVC pipe	X	X	X		
7	pH of outlets and MCW	8.52	7.74	7.72		
8	Conductivity of outlets and MCW (µs/cm)	611	597	597		
9	Sample Taken At (time)	11:22	8:45	8:55		
10	Sampling for Heavy Metals (HM)	X	X	X		
11	Sampling for Sulfate (SO4)	X	X	X		
12	Sampling for total organic carbon (TOC)	X	X	X		

13	Labeling the samples *	X	X	X		
14	Adding preservatives **	X	X	X		
15	Empty the outlets	X	X	X		
16	Temperature of **bioreactors** and MCW (°C)	1.4°C	4.5°C	4.7°C	°C	°C

* Label the samples. For example:

HM MCW - (MM/DD/YYYY) SO4 BR1 - (MM/DD/YYYY) TOC BR1b - (MM/DD/YYYY)

** Use preservatives for each sample : 2% nitric acid for HM and 2% sulfuric acid for TOC

CHECK LIST

1 MCW tank must be emptied and refilled with fresh MCW from Ditch A pipe.
MCW pump must be stopped before emptying and refilling the MCW tank.
MCW tubing pipes should be placed approximately 20 cm from the bottom of the tank.

2 Four tubing pipes must go from the MCW tank to the MCW pump to 4 bioreactors.
Two tubing pipes must go from the molasses solution to the CS pump 1 to the inside bioreactors.
Two tubing pipes must go from the molasses solution to the CS pump 2 to the outside bioreactors.

3 New molasses solution must be prepared weekly.
Automatic stirrer must stir the molasses solution constantly.

4 MCW pump must run constantly.

CS pump 1 and 2 must run from 16:00 to 16:26 everyday.

5 Heater must be always on and set to 5°C.

Annex 3: Spruce wood chips carbon leaching experiment

Materiel and Method:

A column test was installed on November 19th ,2020 in the YukonU Research Center, to assess the total organic carbon (TOC) leaching potential of wood chips used in the Eagle Gold Mine bioreactors. Two columns were installed in duplicates, at room temperature. Each column have a volume of 2000mL. Each column was filled with 20% v/v wood chips (local Yukon white spruce) ranging from 0.3mm to 100.0mm. Deionized water stored in a 18L container was pumped from the bottom to the top of the columns by a peristaltic pump (Masterflex L\S Standard Digital Drives; Cole Parmer Canada, Montreal, QC, Canada). The peristaltic pump was set at 0.08 RPM to achieve a hydraulic retention time of 14 days at 0.08mL/min. The deionized water went from the 18L container, to the columns, to the collection jars (2L glass jars) through tubing (C-Flex L\S 16 tubing; Cole Parmer Canada, Montreal, QC, Canada). The tubing was connected to the columns using fittings (Adapter Fitting Hose Barb to Male NPT Threaded, Cole Parmer Canada, Montreal, QC, Canada) sealed with thread seal tape and silicone. The tubing was connected to a pump head (Masterflex L/S Easy-Load II Pump Head, Cole Parmer Canada, Montreal, QC, Canada) to the peristaltic pump using stop tubing (Masterflex L/S 2-Stop Pump Tubing, Cole Parmer Canada, Montreal, QC, Canada).

Water samples were collected from the collection jars after stirring the water, on a weekly basis. Samples for total organic carbon were preserved with sulfuric acid (2% v/v). Water from the collection jars was removed for the fallowing week samples. Samples were sent to ALS, Whitehorse.

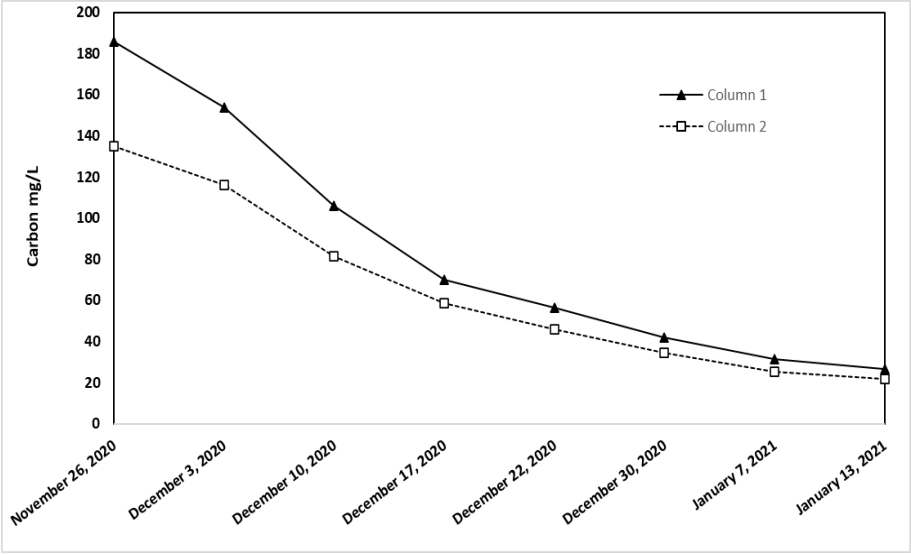

Figure 13: Carbon leaching in column 1 and column 2